ISSN: 1224-7626

ANALELE
UNIVERSITĂŢII DIN ORADEA

Fascicula CHIMIE
XXVI (26)
2019

EDITURA UNIVERSITĂŢII DIN ORADEA

- 2019-

Editor in chief: BADEA Gabriela Elena
gbadea@uoradea.ro

Editors
Gultekin Tarcan – Dokuz Eylul University, Turkey, gultekin.tarcan@deu.edu.tr
Arife Alev Karagozler - Adnan Menderes University, Aydin, Turkey, akaragozler@gmail.com
Cavit Uyanik - Kocaeli University, Kocaeli, Turkey
Hrefna Kristmannsdottir-Efla Engineering Company, Iceland
Jantschi Lorentz- Technical University of Cluj Napoca, România, lorentz.jantschi@gmail.com
Ioniţă Daniela- University Politehnica of Bucharest, România, md_ionita@yahoo.com
Cojocaru Anca- University Politehnica of Bucharest, România, a_cojocaru@chim.upb.ro
Maior Ioana- University Politehnica of Bucharest, România, i_maior@chim.upb.ro
Iovi Aurel - University Politehnica Timişoara, România
Gilău Ludovic – University of Oradea, România
Bungău Simona – University of Oradea, România, simonabungau@gmail.com
Badea Gabriela Elena- University of Oradea, România, gbadea@uoradea.ro
Fodor Alexandrina - University of Oradea, România, afodor@uoradea.ro
Cărăban Alina - University of Oradea, România, acaraban@uoradea.ro
Stănăşel Oana - University of Oradea, România, ostanasel@uoradea.ro
Gavriş Georgeta- University of Oradea, România, georgeta_gavris@uoradea.ro
Hodişan Sorin - University of Oradea, România, sorin.hodisan@yahoo.com
Sebeşan Mioara - University of Oradea, România, msebesan@uoradea.ro
Cozma Alina - University of Oradea, România, acozma@uoradea.ro
Bota Sanda - University of Oradea, România, sbota@yahoo.com
Petrehele Anda - University of Oradea, România, pcorinamara@yahoo.com
Morgovan Claudia - University of Oradea, România, cmorgovan@yahoo.com

Editorial Adress
University of Oradea, Chemistry Departament
Str. Universitatii, nr.1, 410087, Oradea, Bihor, România
General Information
ISSN: 1224-7626
Place of publishing: Oradea, Romania
Year of the first issue: 1995
Releasing frequency: 1 issue / year
Language: English
Abstracting/Indexing:

Chemical Abstracts Service-CAS Source Index (CASSI)

Academic Research Index- ResearchBiB

TABLE OF CONTENTS

NANOSTRUCTURED SURFACES FOR IMPLANTOLOGY-OBTAINING AND CHARACTERIZATION

Andrada Maria NEGRU[1], Mariana PRODANA[2], Matei Maxim POPESCU[2], Bianca Mihaela DIMITROV[2], Daniela IONITA[2]

[1] University of Pitesti, 110040, Pitesti, Romania
[2]University “Politehnica” of Bucharest, 011061, Bucharest, Romania

Abstract
Metallic biomaterials (especially alloys) are mainly used for implants with high mechanical stress (hip, knee) in the form of screws, nails and fracture fixation plates, and in cardiovascular surgery in the form of valves and pacemaker connections. In our paper we obtained a new nanostructured material that contains hydroxyapatite and collagen to facilitate oseointegration obtained like a layer on a titanium alloy

Key words: biomaterials, nanostructured electrode, hydroxyapatite , collagen SEM, FTIR,

INTRODUCTION

Metallic biomaterials (especially alloys) are mainly used for implants with high mechanical stress (hip, knee) in the form of screws, nails and fracture fixation plates, and in cardiovascular surgery in the form of valves and pacemaker connections[1-3].The following alloys are widely used: 316L stainless steel, pure titanium and its alloys, cobalt-chromium-molybdenum alloy [4].

Surface modification of titanium alloys are a good method to improve the its properties with the aim of being further used in implantology, to increase the implant's oseointegration capacity [5, 6]

Nanostructured materials are very important for implantology because surface nanofeatures provide significant potential solutions to medical problems due to its immense surface, improved design of the implant and surface techniques like coatings or functionalization at the nanoscale [7].

The improvement of the bone-forming activity at the bone-implant interface is committed to nanoscale features that have the ability to induce the differentiation of stem cells along the osteogenic pathway [8,9]. Nanotechnology involves the creation of functional materials, devices and systems through control of matter on the nanometer length scale (1–100 nm). The application of nanotechnology to biomedical surfaces is explained by the ability of cells to interact with nanometric features [8].

Calcium phosphate materials have become interesting for medical practice as potential candidates for manufacturing implants in the human body. Calcium phosphates are used to produce artificial bones, but recently, through their synthesis, they are already used to make new types of implants or just as solid layers or processes that cover metallic implants [10, 11].

Collagen it is a structural protein that we find in skin, joints and connective tissue. Collagen is the most common protein in the human body, 35% of total protein is collagen [12].

In our paper we obtained a new nanostructured material that contains hydroxyapatite and collagen to facilitate oseointegration obtained like a layer on a titanium alloy [13].

MATERIALS AND METHODS

For the experimental part we used three Ti50Zr alloy plates with an area of 8 cm^2.This paper intent to modify the surface of these samples by different methods and various treatments, which can facilitate hemocompatibility: hydroxyapatite (HA), collagen (Col).

The titanium samples have the composition as following 50% Zr and Ti rest. These samples were pretreated by metallographic paper, washed with ethanoland withbidistilled water and dried in air.

Before deposition of Col/HA complex we anodized the alloys plates in order to obtain a nanostructuration of the surface. After anodization we deposited a Col/HA by two different methods: electrodeposition and spin coating method.

Electrodeposition of Collagen/HA on TiO_2 nanotubes complex deposited on alloys plates was performed from an aqueous suspensions. The deposition was presented with its steps in a previous work [14].

The microstructure characterization of the reference anodized material and hybrid complex ceramic coating was studied by optical method using an *Carl Zeiss AXIO Scope A1 microscop* and scanning electronic microscopy (SEM) using the Microscope Hitachi SU 8230 coupled with and EDAX (energy dispersive spectra) module.

The hydrophilic/hydrophobic balance was estimated using a CAM100 contact anglemeter in order to evaluate the chance of good biocompatibility of these samples.

Electrochemical measurements for reference and for coated Ti sample were carried out using a VoltalabPotentiostat/ Galvanostat PGZ 301 equipped with Volta Master Sofware. The system used for electrochemical tests was a three electrode cell with a reference electrode Ag/AgCl (3M), working electrode as Ti50Zr coated and anodized samples and Pt as a counter electrode.

The structure of the samples was identified with Fourier Transformed Infrared (FTIR) spectroscopy using an ATR system Spectrum 100 equipment in 500÷4500 cm^{-1} range with 4 cm^{-1} resolution and 32 scans from Perkin Elmer Company.

Anodic oxidation (anodization) is the electrochemical method of forming high oxide layers and a particular structure in specific reaction media. The process consists in the anodic polarization of an electric circuit on the biomaterial surface (Ti50Zr in our case) in a well-chosen solution.

As a result of this anodizing process, layers of oxide of different sizes have formed on the surface of Ti50Zr plates, which have an important role against corrosion, which can seriously affect the body.

The exposed area of the samples to electrolyte test solution which is SBF was 1 cm^2. The SBF composition is the subject of table 1.

Table 1. SBF chemical composition (g/L)

NaCl	KCl	$CaCl_2$	$NaHCO_3$	Na_2HPO_2 $2H_2O$	$MgCl_2$ $6H_2O$	KH_2PO_4	$MgSO_4\cdot$ $7H_2O$	Glucose
8	0.4	0.18	0.35	0.48	0.10	0.06	0.10	1

Three samples were anodized, Sample 1 was kept as a standard-reference sample, and the other two were used in subsequent experiments (for HA and collagen deposition by two different methods: Electrochemical and Spin Coating).

The anodization was made under the following conditions: A current of -21mA was used and left the Ti50Zr plate anodized for 30 minutes in an electrolyte formed from 6.3 ml of 85% H_3PO_4 and 0.5 ml of H_2O.

As a result of this anodizing process, layers of oxide of various sizes were formed on the surface of the Ti50Zr plates.

For Sample 2, electrochemical deposition of HA and collagen was performed by chronoamperometric method on a previously anodized Ti50Zr plate.

For Sample 2 we selected -1.4V vs. Ag / AgCl for two hours, and a new electrolyte solution was prepared with HA: 42 mM Ca $(NO_3)_2$ + 25 mM $NH_4H_2PO_4$ (9.91 Ca $(NO_3)_2$* H_2O + 2.875 $NH_4H_2PO_4$ / 1L H_2O) 1% collagen solution (collagen was dissolved in acetic acid solution).

For sample 3, on an anodized Ti50Zr plate, we applied the Spin Coating process; the mixture of HA and collagen was deposited on the surface of the anodized Ti50Zr plate.

The method consists of applying thin films on flat substrates. Thus, a large amount of solution is applied to the substrate, which is rotated at very high velocities, the fluid enveloping the substrate under the action of centrifugal force. The thickness of the film ultimately depends on both the angular velocity and the concentration of the solution and the solvent. This method produces layers with thicknesses below 10 nm.

Characterization of the samples:

MO - optical microscopy uses light radiation resulting in a larger, virtual or real image of objects prepared in a suitable manner.

By the MO we can see dimensions of the order μm. Figure1 presents the images for optical microscopy obtain for all the samples.

The morphology of samples 1, 2 and 3 is observed.For sample 1 a porous structure is observed. For samples 2 and 3, there is visible the deposition of hybrid material made up of HA and Collagen.

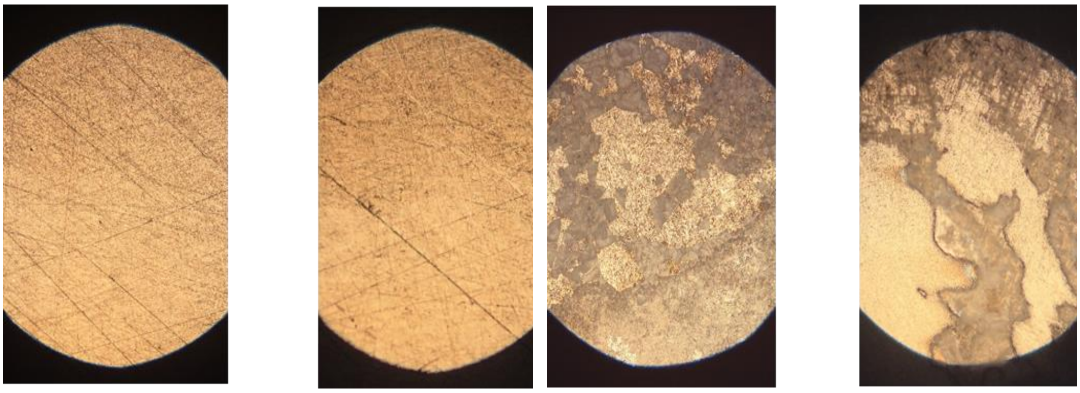

a) Sample 1 b) Sample 2

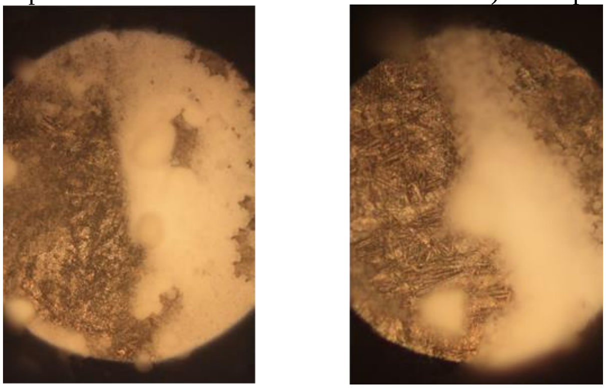

c) Sample 3

Figure 1. Optical microscopy images

Contact angle measurement (CA)

This method is an accurate assessment of hydrophilic / hydrophobic balance for titanium alloy samples.

In Figure 2 we can see the values obtained for every samples.

We obtained that all samples are very hydrophilic. The value of the contact angles obtained is very close to the three analyzed samples (12.90, 17.35, 12.40 degrees).

Fourier Transform Infrared Spectroscopy (FTIR)

Infrared (IR) spectroscopy is the most appropriate method for identifying the presence of polar functional groups in the structure of the molecules of organic compounds.For recording the IR spectra used to determine the structure of organic compounds, only the middle IR range containing wavelengths in the 2.5-25 μm region is used (most often the characterization is done using wavelengths ranging from 400-4000 cm^{-1}). In Figures 3 is presented the FTIR spectra obtained for our samples.

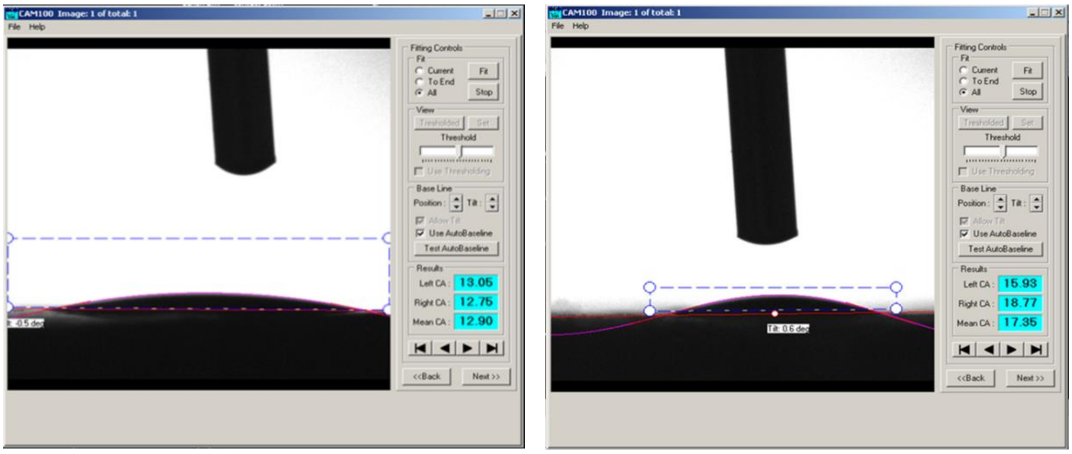

Tilt: -0.5 deg

Left CA : 13.05
Right CA : 12.75
Mean CA : 12.90

Tilt: 0.6 deg

Left CA : 15.93
Right CA : 18.77
Mean CA : 17.35

a) Sample 1 b) Sample 2

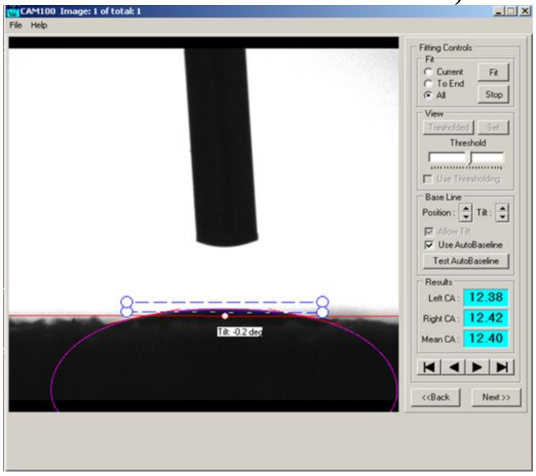

Tilt: -0.2 deg

Left CA : 12.38
Right CA : 12.42
Mean CA : 12.40

c) Sample 3

Figure 2. Contact angle measurements for samples

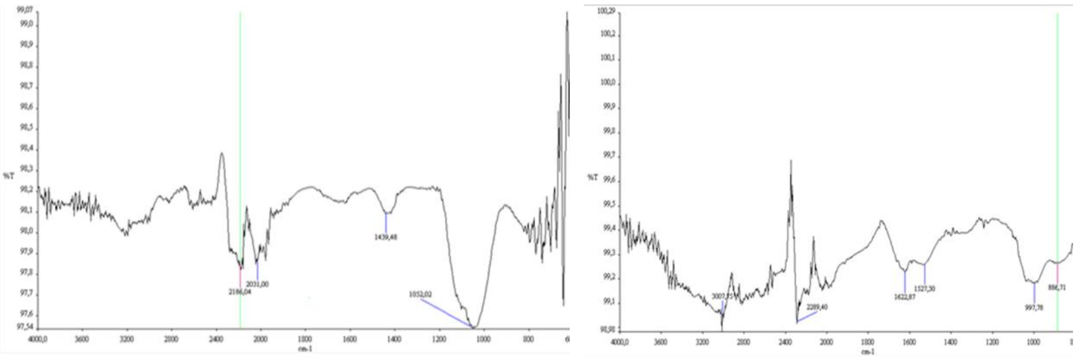

a) Sample 1 b) Sample 2

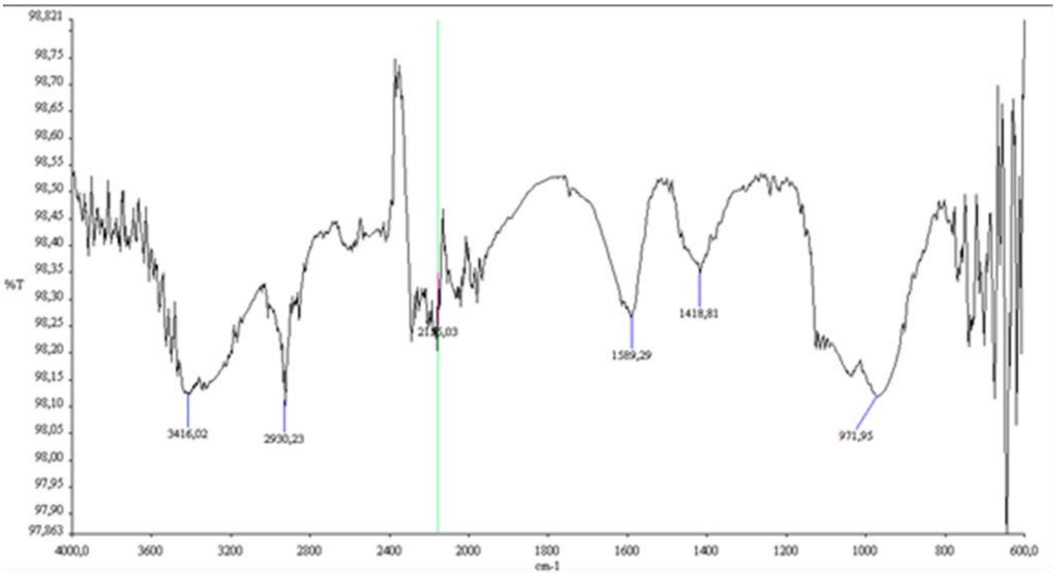

c) Sample 3

Figure 3. FTIR spectra of the samples.

Four representative peaks are obtained, the attributes of which are in the table 2. The -PO4 group comes from the electrolyte used for anodizing.

Electronic Scanning Microscopy (SEM) coupled with X-ray diffraction spectra (EDAX)

SEM is a type of electron microscopy that produces images by scanning the sample surface with a concentrated electron beam.

High energy electrons interact with the analyzed material and dissipate into a number of forms of energy that include: secondary electrons and retro-diffused electrons that are used to create morphological images, X-rays specific for elemental analysis, visible light and heat.SEM can record nm-μm dimensions

Figures 4, 5 and 6 presents the morphology and the spectra of the samples.

For sample 1 a porous morphology is observed.EDAX confirms the existence of Ti and Zr oxides.

For sample 2, grains of HA + Col hybrid material are obtained. The deposition shows cracks and in the EDS spectrum there appear the Ti and Zr peak.EDAX highlights existing HA with Ca / P = 1.6.

Table 2: FTIR attributed wave length

Sample 1 wave number (cm^{-1})		Sample 2 wave number (cm^{-1})		Sample 3 wave number (cm^{-1})	
1052	$-PO_4$	997	P=O	971	P=O
1439	-OH	1527	-NH	1418	CO_3^{2-}(from atmosphere)
2031	the vibration of the -OH adsorbed group coupled with Zr^{4+}	1622	CaCOO- (specific for collagen)	2156	CO_3^{2-}
2186	due to the absorbed water molecules	2289	H_2bond absorbed from H_2O	2930	H_2bond absorbed from H_2O
-	-	3007	-OH (hydroxyl)	3416	OH^- (typical for HA)

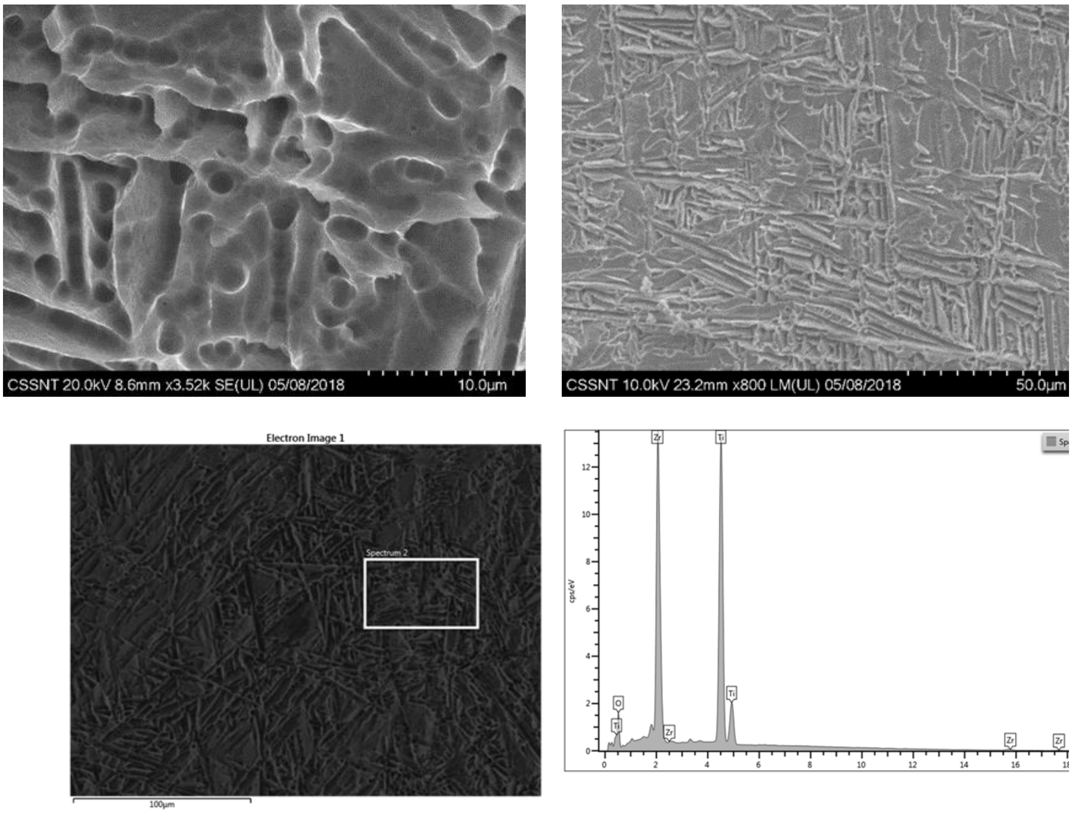

Figure. 4. Morphology and EDAX for sample 1

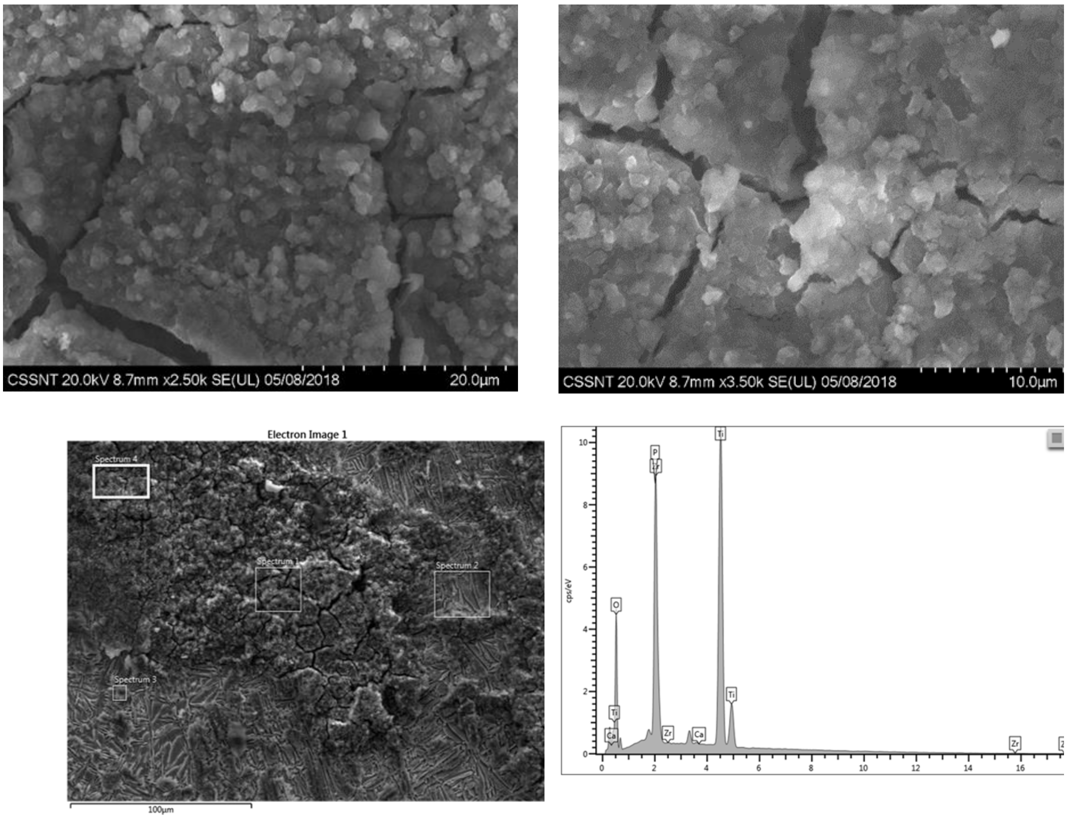

Fig. 5. Morphology and EDAX for sample 2

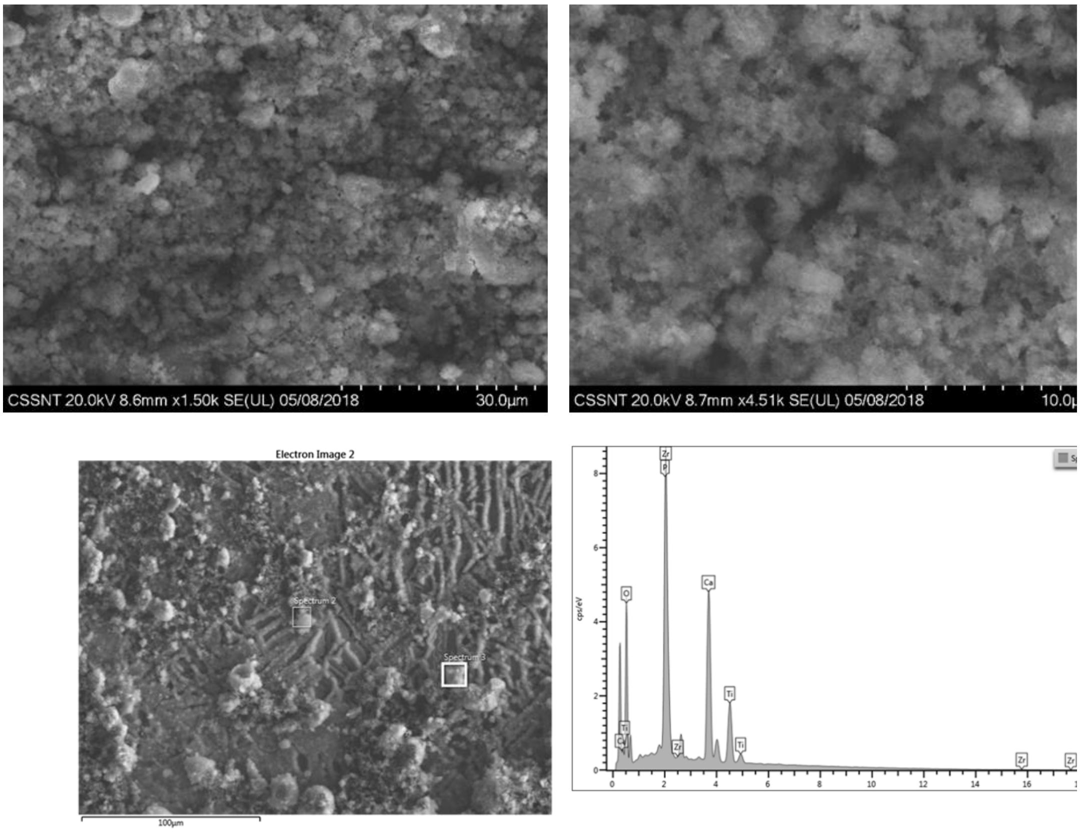

Figure 6. Morphology and EDAX for sample 3

CONCLUSIONS

By optical microscopy measurements the surface of the samples was visualized at different magnifications. For Samples 2 and 3, the presence of hybrid material is visible.

From the FTIR determinations it was revealed that for Samples 2 and 3, similar peaks were obtained at very close wavelengths between them, which highlighted the coverage with the same material, a composite material composed of HA and collagen.

The hydrophilicity of the samples was determined from the angle of contact measurements. All samples have a small contact angle, very close to the value (12-17.5 °).

Following the SEM measurements, the morphology of the samples was determined. For Sample 1, the presence of a porous titanium oxide and zirconium oxide layer is observed on the surface of the titanium alloy. In Probe 2, a morphology specific to electrochemical deposition of HA and collagen was obtained in the form of nearly circular shaped structures. For Sample 3, sample morphology indicates the existence of HA and collagen deposits in a circular form, very similar to those obtained for Sample 2.

From the EDAX measurements, there was a layer of Zn O and TiO2. For both sample 2 and sample 3, a Ca / P = 1.6 ratio of hydroxyapatite.

REFERENCES

[1] Acero, J., Calderón, J., Salmeron, J.,Verdaguer, J., Consejo, C. (1999). The behaviour of titanium as a biomaterial: microscopy study of plates and surrounding tissues in facial osteosynthesis. Journal of Cranio-maxillofacial Surgery; Vol.27 (2), pp. 117-123.

[2] Dadvinson, A., Gergette, F. (1986). State of the art in materials for orthopedic prosthetic devices. Proceedings of Implant Manufacturing and Materials Technology. Soc. Manufact. Eng., Em87-122, pp. 122-126.
[3]Katti, K. (2004). Biomaterials in total joint replacement. Colloids and Surfaces B: Biointerfaces; Vol.39 (3), pp. 133-142.
[4] Rao, S.,Ushida, T.,Tateishi, T., Okazaki, Y., Asao, S. (1996). Effect of Ti, Al, and V ions on the relative growth rate of fibroblasts (L929) and osteoblasts (MC3T3-E1) cells. BioMedical Materials and Engineering; Vol.6 (2), pp. 79-86.
[5]Le Guéhennec, L., Soueidan, A., Layrolle, P., Amouriq, Y. (2007). Surface treatments oftitanium dental implants for rapid osseointegration. Dent Mater OffPublAcadDent Mater; Vol. 23, pp. 844–854.
[6] Junker, R., Dimakis, A., Thoneick, M., Jansen, J.A. (2009). Effects of implant surface coatingsand composition on bone integration: a systematic review. Clin Oral ImplantsRes; Vol 20 (4), pp. 185–206.
[7]Rahimeh, R., Ahmed, B., Hasan, U. (2018). A review of nanostructured surfaces and materials for dental implants: surface coating, patterning and functionalization for improved performance. Biomaterials Science; Vol. 6 (6), pp. 1-72
[8] Bressan,E., Sbricoli, L., Guazzo, R., Tocco, I., Roman,M., Vindigni, V., Stellini, E., Gardin, C., Ferroni, L., Sivolella,S.,Zavan, B. (2013). Nanostructured Surfaces of Dental Implants. Int. J. Mol. Sci.: Vol. 14, pp. 1918-1931.
[9] Variola, F., Yi, J.H., Richert, L., Wuest, J.D., Rosei, F.,Nanci, A. (2008). Tailoring the surface properties of Ti6Al4V by controlled chemical oxidation. Biomaterials; Vol. 29, pp. 1285–1298.
[10]Weng, J., Liu, X., Zhang, X., Ji, X. (1994). Thermal decomposition of hydroxyapatite structure induced by titanium and its dioxide. Journal of Material Science Letters, Vol.13 (3), pp. 159-161.
[11]Yang, Y., Kim, K., Agrawal, C., Ong, J. (2004). Interaction of hydroxyapatite-titanium at elevated temperature in vacuum environment. Biomaterials; Vol.25 (15), pp. 2927-2932.
[12] Herford, A.S.,Akin,L.,Cicciu, M., Maiorana, C.,Boyne,P.J. (2010). Use of a Porcine Collagen Matrix as an Alternative to Autogenous Tissue for Grafting Oral Soft Tissue Defects, Journal of Oral and Maxillofacial Surgery;Vol. 68 (7), pp. 1463-1470.
[13] Zhiguang, L.,Yumei, Z.,Huan, S.,Lijuan, X.,Yuyong, C., Woo, K. (2009). Porous Ti/HA biocomposites for biomaterials applications. Materials Science Forum; Vol.614, pp. 73-78
[14].Prodana, M.,Duta,M.,Ionita,D.,Dinischiotu, A.,Demetrescu,I. (2015). A new complex ceramic coating with carbon nanotubes, hydroxyapatite and TiO_2 nanotubes on Ti surface for biomedical applications. Ceramics International; Vol. 41 (50), pp. 6318-6325.

Analele Universităţii din Oradea-Fascicula Chimie, Vol. XXVI(26), 2019

IRON (II) SPECTROFOTOMETRIC DETERMINATION IN SPINACH (*SPINACIA OLERACEA*) FRESH LEAVES AND SPIRULINA (*ARTHROSPIRA PLATENSIS*) POWDER

Alexandrina FODOR[1], Anda Ioana Graţiela PETREHELE[1], Claudia MORGOVAN[1], Teodora SOCA[2]

[1] University of Oradea, Romania, Oradea, 418070, Str. Universităţii no. 1, afodor@uoradea.ro
[2] University of Oradea, Faculty of Informatics and Sciences, Master CSA I -Student

Abstract: *The determination of the iron content in two important components of the vegetarian diet (fresh Spinach leaves and Spirulina powder) were performed using spectrophotometrical method, using as colour indicator* o-o'-phenanthroline *($C_{12}H_8N_2$), at pH = 4-5 and 510 nm. The results indicated that Spirulina contains a much larger amount of Fe (II) than spinach (7.42 times higher).*

Key words: Spinacia Oleracea fresh leaves, Arthrospira Platensis powder, UV-VIS Spectrophotometric determination, o-o'-phenanthroline

INTRODUCTION

Iron plays an important role in biochemistry, forming molecular oxygen compounds in hemoglobin and myoglobin; two compounds which are common proteins that play role in the transport of oxygen in vertebrates body's. Iron is also the metal most commonly used by the most important redox enzymes, which are involved in cellular respiration, oxidation and reduction processes in plant and animal organisms [1].

Iron is an essential mineral for the human body. The iron source for animal organisms is the intake food and is lost through the continuous exfoliation of the cells of the digestive tract, urinary tract and skin cells. It is stored in the form of ferritin in the cells of the spleen, liver and bone marrow, and another part circulates in blood bounded to transferrin (a transport protein specific to iron) [2].

The importance of iron in the human body derives depending on the quantity in which it is found. The human body needs a consistent contribution to fulfil its functions. Iron must exist at the highest level to meet all needs [2].

Iron deficiency is the result of reduced consumption of iron containing foods (in the case of the vegetarian diet for example) and of some diseases that impede its absorption. The most important sources of iron for the human body are red meat and liver. In the case of a vegetarian diet to ensure the amount of iron necessary for the body, high-iron plant foods such as some seeds, vegetables and fruits should be included in the diet [3].

Two important components of the vegetarian diet, used as sources of Fe, fresh Spinach (*Spinacia Oleracea*) fresh leaves and Spirulina (*Arthrospira Platensis*) powder, were investigated in terms of the Fe (II) content.

The determination of the iron content was performed using spectrophotometrical method, using as colour indicator o-o'-phenanthroline ($C_{12}H_8N_2$), at pH = 4-5 and 510 nm, based on the reaction [4]:

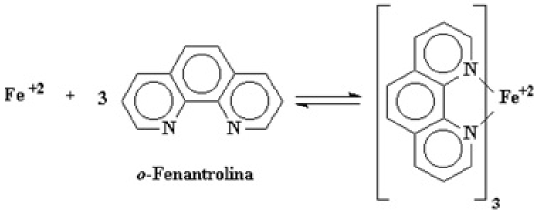

Figure 1. Fe(II) reaction with o-o'-phenanthroline

MATERIALS AND METHOD

The used method was the spectrophotometric determination using the etalon scale method.

The used reagents were: deionised water solution of: 25% sodium acetate, 10%, hidroxilamine clorohydrat, 0,5 % ethanol alcoholic solution of o-o'-phenanthroline, H_2SO_4, Fe (II) etalon solution for the etalon scale preparation (1-5 mg Fe (II)/L) 25 mg/L Fe(II) (prepared by dissolving 67.96 mg $FeSO_4$ in 25 mL distilled water acidified with H_2SO_4).

For the spectrophotometric analysis a Spectrophotometer Vis Jenway 6320D, 320 - 1000 nm were used.

Sample preparation

The spinach *(Spinacia Oleracea)* fresh leaves were placed in an oven (at 1000 ^oC) for 1 hour in order to determine the humidity. The humidity of the sampled spinach leaves was 76,84%. The dried leaves were wetted to be subsequently treated for Fe (II) extraction.

Spirulina *(Arthrospira Platensis)* was purchased in powder form therefore does not require drying and soaking.

5 g of samples powders (Spinach and Spirulina), were place in porcelain capsules and place in a calcining oven at 500 ^oC for one hour. The obtained powders were moistened with 5 drops of sulphuric acid and taken with distilled water in small portions, filtered and passed into 50 ml graduated flasks and brought to the mark with distilled water.

F**or the Spinach sample:** 10 ml of sample solution were taken from the flask and pass into a 25 ml flask and brought to the mark with distilled water.

For the Spirulina sample: 1 ml of sample solution was taken and passed into a 25 ml graduated flask and brought to the mark with distilled water.

Higher dilution is practiced in the case of Spirulina due to the fact that in the literature it is stated that Spirulina contains higher quantities of Fe (II) than Spinach [8]

The following reagents (same reagents as for the standard scale) are added to the two samples:

- 5 ml 25% sodium acetate
- 1 ml 10% hydroxylamine chlorhydrat,
- 1 ml 0,5 % ethanol alcoholic solution of o-o'-phenanthroline.

The added solutions were stirred well, distilled water was added to the mark and then the obtained mixture was leave to stand for 1 hour.

The blank solution was prepared from:

- 5 ml 25% sodium acetate
- 1 ml 10% hydroxylamine chlorhydrat,
- 1 ml 0,5 % ethanol alcoholic solution of o-o'-phenanthroline.

The added solutions were stirred well, distilled water was added to the mark and then the obtained mixture was leave to stand for 1 hour.

The standard solutions (standard scale), consisting in 10 Fe (II) solutions with concentrations between 1-5 mg/L are prepared as follows:

In 10 25 ml graduated flasks were added:

- 5 ml 25% sodium acetate
- 1 ml 100,5 % ethanol alcoholic solution of o-o'-phenanthroline.
- 1,2,3,4 and respectively 5 ml Fe (II) etalon solution (25 mg/L)

The added solutions were stirred well, distilled water was added to the mark and then the obtained mixture was leave to stand for 1 hour.

All the spectrophotometric determination was performed at 510 nm.

RESULTS

By graphically representing the result of the measurement of the absorbance for the standard scale, the right of calibration is obtained:

The measured absorbance's for the investigated samples were presented in figure 2.

The amounts of Fe(II) determined for spinach and spirulin samples from the interpolation on the calibration curve are:

Spinach: 3,6245 mg/L
Spirulin: 3,5021 mg/L

Calculus:Spinach

1000 ml……3,6245 mg/L mg Fe(II)
10 ml…………………x
x= 0,036245 mg Fe(II)

taking into account the dilution: 0,036245 · 50 = 1,81225 mg Fe(II) în dried leaves

taking into account the moisture of the Spinach leaves: 1,81225 · 100/76,84= **2,35847 mg Fe(II) in 100 g fresh Spinach leaves**

Calculus:Spirulin
1000 ml………3,5021 mg/L mg Fe^{+2}
10 ml…………………x
x= 0,035021 mg Fe(II)
taking into account the dilution: 1,75105·500= **17,5105 mg Fe(II) in 100g Spirulina powder**

The results are in good agreement with the data from the literature (3,8 mg Fe (II) in 100 g fresh Spinach leaves and respectively 28 mg Fe(II) in 100 g Spirulina powder)[4].

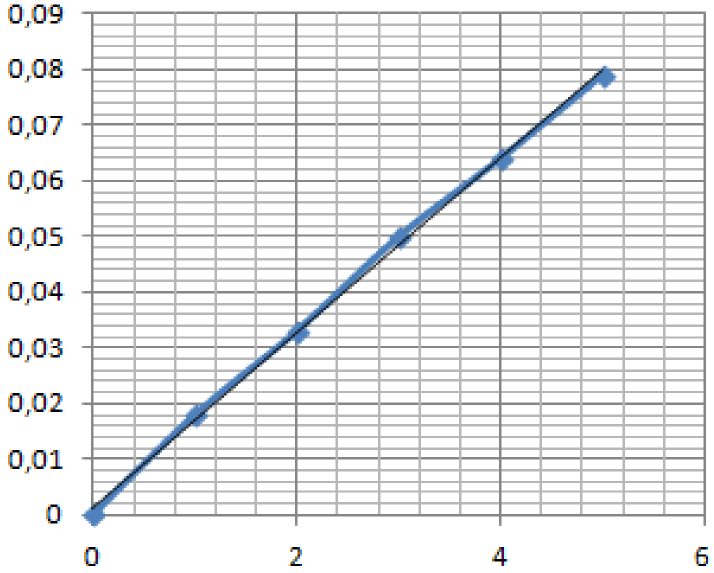

Figure 2. Calibration curve for the determination of the Fe (II)

Table 1. The absorbance's measured for the spinach leaves samples and for the spiruline samples

	Absorbance Determination 1	Absorbance Determination 2	Absorbance Determination 3	Absorbance Average
Spinach *(Spinacia Oleracea)*	0,0563	0,0564	0,0561	0,0562
Spirulina *(Arthrospira Platensis)*	0,0498	0,0497	0,0499	0,0498

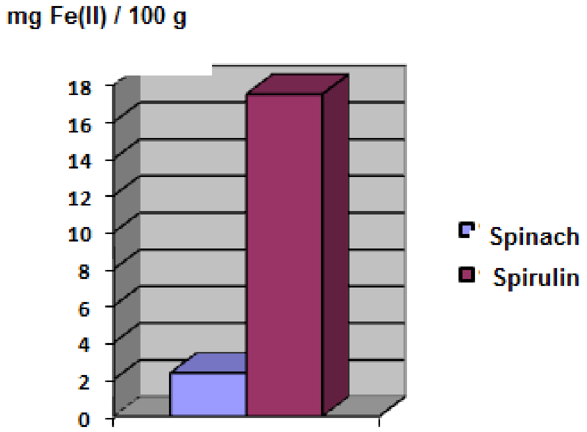

Figure 3. Fe (II) content in the samples of fresh Spinach leaves and Spirulina powder

CONCLUSIONS

The spectrophotometric method for the determination of Fe(II) for the two plant samples proved to be a laborious method (it required numerous operations such as drying, calcining, weighing, diluting, preparing the Fe(II) standard scale, etc.) but inexpensive.

The results are in good agreement with the data from the literature [4].

It can be seen that Spirulina powder contains a much larger amount of Fe (II) than Spinach fresh leaves (7.42 times higher).

Considering that the daily iron requirement for an human adult is approx. 2 to 5 mg. Thus, according to the results of the study, it is recommended for people on a vegetarian (vegan) diet to consume about 40 g of fresh Spinach leaves daily or about 4 g of Spirulina powder.

REFERENCES

[1] L., Ghizdavu, Chimie bioanorganică, Editura Poliam Cluj-Napoca, 2000
[2] A., Găman, G., Găman, Explorarea metabolismul fierului, INFOMedica 1998, (8), pp. 54
[3] R. Eliliot, The Vegetarian Low-Carb Diet, Piatkus Book, UK, 2005
[3] L. D. Harvey, Modern Analytical Chemistry, McGraw-Hill, 2000
[4] USDA Food Composition Databases-https://ndb.nal.usda.gov/ndb/h, 08.01.2020

SYNTHESIS AND CHARACTERIZATION MESOPOROUS MAGNETITE IN THE PRESENCE OF BUBBLING NITROGEN

Ioana Lavinia ARDELEAN[1], Luric Bogdan NICULAE STOENCEA[2],
Adrian Ionuț NICOARĂ[2], Roxana TRUȘCĂ[2], Gheorghe NECHIFOR[2]

[1]University of Oradea, Department of Chemistry, Romania, dy4_ioana@yahoo.com
[2]University Politehnica of Bucharest, Faculty of Applied Chemistry and Material Science;
1-7 Polizu St., Bucharest, Romania,

Abstract:

In this paper the synthesis of magnetic ferrite nanoparticles using nitrogen bubbling as stabilizer agent is presented. Co-precipitation methods was used to obtained magnetic ferrite nanoparticle. To determine the structure and morphologies of both types of iron ferrite nanoparticles, with and without nitrogen bubbling were used as methods of analysis: X-ray diffraction (XRD), Fourier transform infrared spectroscopy (FTIR), scanning electron microscopy (SEM) and -Emmett-Teller (BET). The Brunauer-Emmett-Teller analysis (BET) shows a mesoporous structure of the magnetic nanoparticles with specific surface area of approximately 156m^2/g in the case of stabilized magnetite and an increase of about 166 m^2/g in the case of nitrogen bubbling magnetite. The average pore size increases from 5.75 nm for magnetite, to 6.79 nm for bubbled nitrogen magnetite.

Keywords: co-precipitation methods, magnetic ferrite nanoparticles.

INTRODUCTION

Technological developments taking place in recent years have shown that magnetic ferrite nanoparticles are of particular interest in medicine (magnetic resonance imaging, drug delivery system, hyperthermia), engineering, biotechnology, etc. Due to their magnetic properties they have been used in biomedical applications due to the low of toxicity, good biocompatibility, long durability[1-6].

Studies on magnetite nanoparticles have shown that the most efficient method of obtaining magnetic nanoparticles is the coprecipitation method due to low costs. Iron ferrite nanoparticles were also obtained by methods such as: sol-gel, hydrothermal, thermal decomposition[1,5-8].

Wei and collaborators obtained iron ferrite nanoparticles using oleic acid and sodium citrate as a stabilizing agents.. The result of the analyses proved a good dispersion, but also a decrease of the magnetization[9].

Antal and collaborators obtain magnetite nanoparticles functionalized with lysine, using as a lysine stabilizing agent. D, L-lysine being considered to be a promising candidate in antibody conjugation[10].

In order to obtain the magnetite nanoparticles in this paper, the coprecipitation method was used as the working method. In this study nitrogen bubbling was used as stabilizing agent. The obtained nanoparticles were analyzed from the point of view of the degree of magnetization, crystallinity, specific surface and size.

EXPERIMENTAL DETAILS MATERIAL AND METHODS

The following materials were used for the preparation of magnetite nanoparticles: ammonium iron(II) sulfate hexahydrate – $Fe(NH_4)(SO_4)_2$ (Silal Trading), iron (III) chloride – $FeCl_3$ (Sigma Aldrich), sodium hydroxide - NaOH (Silal Trading), nitrogen, and distilled water. The magnetic ferrite nanoparticles with bubbling nitrogen were prepared used co-preciptation methods, as presented in Figure 1.

The precipitation solution was prepaired by disolving 10 g NaOH in 250 mL distiled water under mechanical stirring and nitrogen bubbling, at room temperature. The pH was adjusted to 12 and maintained over 10 during precipitation by adding sodium hydroxide solution. The precursors of the magnetite are added by continuous stirring by spraying, at about 3 mL/min. After precipitation the magnetic nanoparticles were filtered and washed three times with distilled water until a neutral pH and free of chloride ions. The magnetic nanoparticles were freeze-dried to avoid further oxidation.

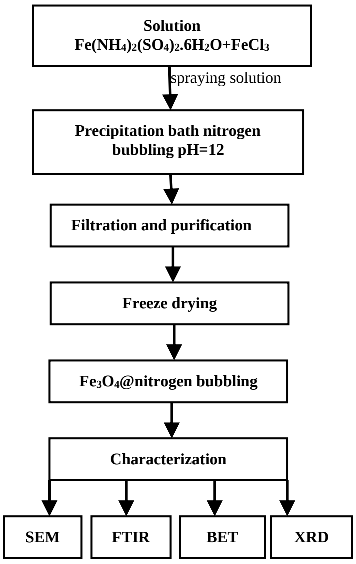

Figure 2. The synthetic steps of Fe_3O_4@nitrogen bubling

The mesoporous magnetic samples were characterized by: FT-IR, SEM, BET and XRD.

RESULTS AND DISCUSSION

➢ *X-ray diffraction*

X-ray diffraction (Figure 1) was used for these nanoparticles to observe the crystallinity, but also the average size of the crystallite.

According to the obtained results it can be seen that the nanoparticles obtained shows peaks specific for spinel cubic structure, and peaks were indexed as *the* planes (220), (311), (400), (422), (511) and (440) which are characteristic for magnetite 17,18,19 (ICDD database).

XRD pattern for Fe3O4 @ nitrogen bubbling shows the same peaks as Fe3O4, but low intensity peaks are not clearly highlighted particularly because of the grain size.

➢ *BET analysis*

The BET analysis was used for evaluate the pore size and surface area of the magnetic nanoparticles.

The BET surface areas of the two samples are summarized in Table 1.

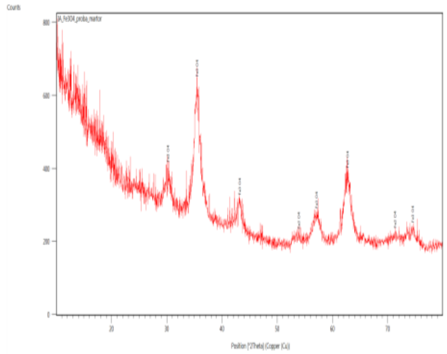

Figure 3. The XRD patterns of the synthesized Fe_3O_4

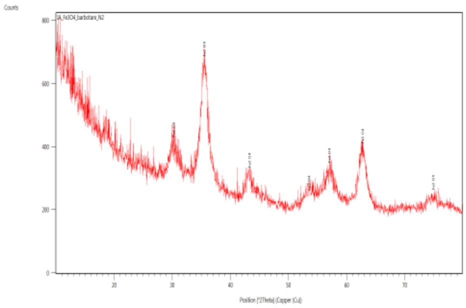

Figure 4. The XRD patterns of the synthesized Fe_3O_4@nitrogen bubbling

According to BET analysis on the simple iron ferrite, there is a specific surface area of 156m^2/g and an average pore size of 5.75 nm. In comparison with stabilized iron ferrite which lead to an increase of the specific surface area of 167 m^2/g and an increase in pore size to 6.79 nm.

The different behavior is explained on the basis of the presence of nitrogen in the magnetite structure.

Based on these data we can conclude that the mechanism of the formation of the Fe_3O_4@stabilizing agent is strongly dependent on the nature of the stabilizing agent the concentration and pH.

Table 1. BET data of the synthesized MNPs samples

Samples	**Specific surface area S_{BET} (m^2/g)**	**Average pore size D_{BET} (nm)**
Fe_3O_4@nitrogen bubbling	166.8264	6.7909
Fe_3O_4@sample	156.0278	5.7466

➢ *Magnetization*

According to the results obtained regarding the degree of magnetization (figure 4) of the nanoparticles is observed that in the case of magnetite sample with nitrogen bubbling is 4.6009 degree of magnetization emu, versus 1.3343 in the case of simple magnetite, that drive an increase in the magnetization due to bubbling with nitrogen.

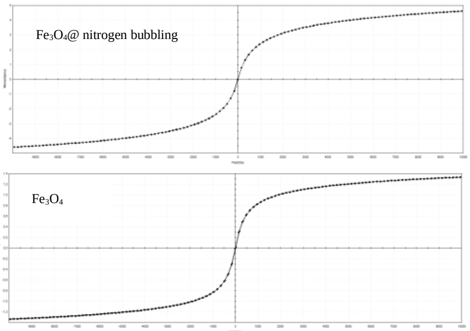

Figure 4. Magnetization curves for iron ferrite nanoparticles with nitrogen bubbling

➢ *Infrared spectroscopy*

FTIR spectra of Fe_3O_4 and Fe_3O_4 @ nitrogen bubbling (Figure 5) shows bands main characteristic absorption magnetite, especially the two peaks intense at 529 and 532 cm^{-1}, due to the stretching mode of vibration associated with the Fe - O bonds in the crystalline Fe_3O_4.

Absorption bands between 1000 and 1650cm^{-1} corresponding to the bending vibration of H-O-H, the molecule typically associated with H_2O adsorbed on nanoparticles surface.

The absorption bands between 1507 cm^{-1} and 900 cm^{-1}, respectively are characteristic O-H in plan.

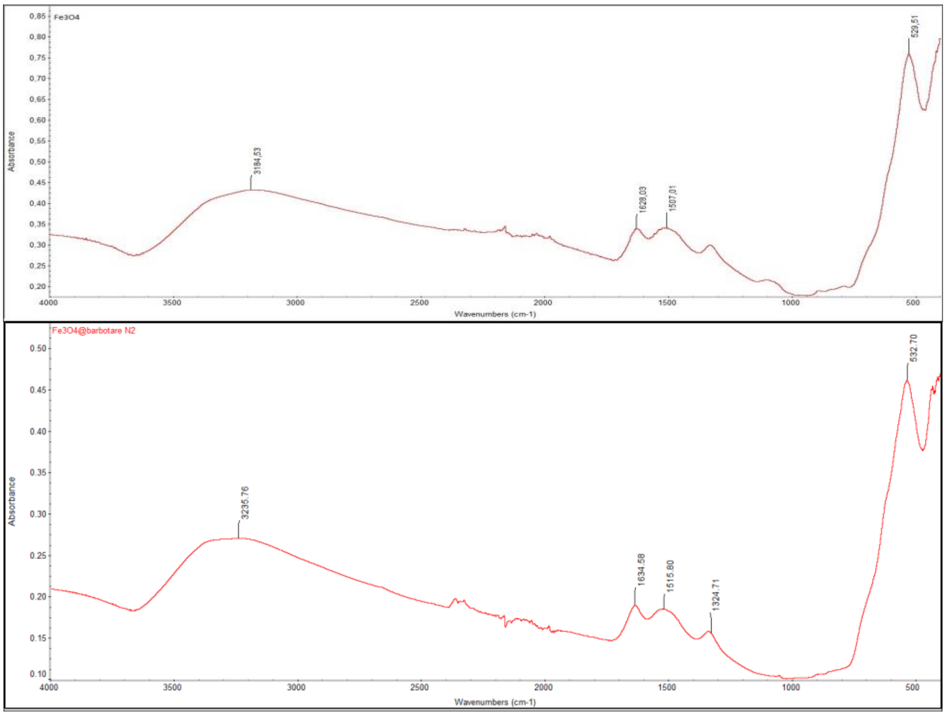

Figure 5. FTIR spectra of the magnetic samples: Fe_3O_4 and Fe_3O_4@nitrogen bubbling

➢ *SEM*

The representative SEM images of the Fe_3O_4 and Fe_3O_4@nitrogen bubbling are presented in Figure 6.

Based on the images, different morphologies of the nanoparticles can be observed due to the presence of nitrogen. Nanoparticle size is in the range of 4-10 nm.

Due to the stabilizing agent, agglomerates can be observed due to the influence of the nitrogen molecule.

Fe_3O_3@ nitrogen bubbling	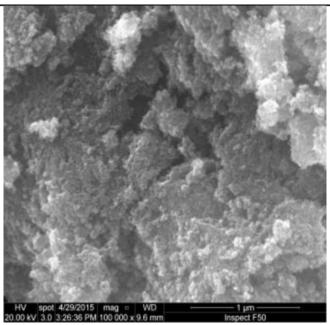	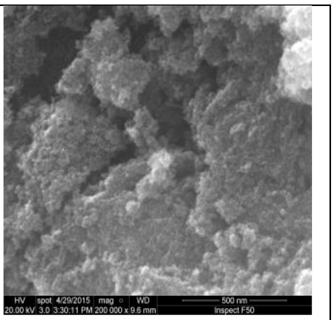
Fe_3O_4	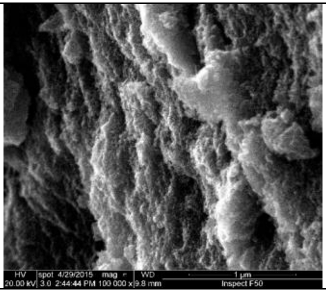	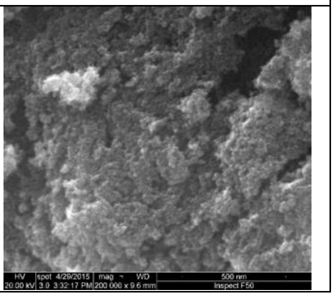

Figure 6. SEM images of the stabilized and non-stabilized magnetic nanoparticles

CONCLUSION

Magnetic nanoparticles were obtained by co-precipitation from the magnetite precursors and bubbling with nitrogen as the stabilizing agent, by spraying the solution of precursor magnetite in alkaline solution stabilizing agent. The obtained results show a difference between Fe_3O_4 and Fe_3O_4 @ nitrogen bubbled nanoparticles. The mechanism of formation of these superstructures is strongly correlated with the presence of a nitrogen molecule, and so the morphological changes occurring in the case of Fe_3O_4 @ nitrogen bubbled comparing with Fe_3O_4.

REFERENCES

1. D.C. Culiță, G.M.L. Patron (2009) Magnetita eternă enigmă; ed. M. ROM., București.

2. L. Mohammed et al. (2017) Magnetic nanoparticles for environmental and biomedical applications: A review. Particuology; 30: 1-14;

3.R. Jurgons, C. Seliger, A. Hilpert, L. Trahms, S. Odenbach, C. Alexiou (2006), Drug loaded magnetic nanoparticles for cancer therapy; Journal of Physics: Condensed Matter, 18 (38): S2893-S2902

4. Y.H. Zheng et al. (2006) Synthesis and magnetic properties of Fe_3O_4 nanoparticles. Materials Research Bulletin. 41(3): 525-529.

5. P. Arevalo et al. (2017) Magnetic and structural studies of Fe_3O_4 nanoparticles synthesized via coprecipitation and dispersed in different surfactants. Ceramics International. 43(13): 10333-10340.

6. A. Elrahman, A.A., F.R. Mansour (2019) Targeted magnetic iron oxide nanoparticles: Preparation, functionalization and biomedical application. Journal of Drug Delivery Science and Technology. 52: 702-712.

7. K.K. Kefeni, T.A.M. Msagati, B.B. Mamba (2017) Ferrite nanoparticles: Synthesis, characterisation and applications in electronic device. Materials Science and Engineering B-Advanced Functional Solid-State Materials, 215: 37-55.

8. I.L. Ardelean et al. (2017) Development of Stabilized Magnetite Nanoparticles for Medical Applications. Journal of Nanomaterials.

9. Y. Wei et al. (2012) Synthesis of Fe3O4 nanoparticles and their magnetic properties. 2011 Chinese Materials Conference, 27: 632-637.

10. I. Antal, M.K., M. Kubovcikova, V. Zavisova, I. Khmara, D. Lucanska, L. Jelenska, I. Vidlickova, M. Zatovicova, S. Pastorekova, N. Bugarova (2017) D,L-Lysine functionalized Fe_3O_4 nanoparticles for detection of cancer cells. Colloids and Surfaces B: Biointerfaces.

Analele Universităţii din Oradea-Fascicula Chimie, Vol. XXVI(26), 2019

THE INFLUENCE OF STORAGE CONDITIONS ON THE ACTIVITY OF INSULIN ASPART

Oana Delia STĂNĂŞEL[1], Alina Maria CĂRĂBAN[1], Sergiu Robert SIMA[2]
[1]University of Oradea, University Str. no.1, 410087
[2]University of Oradea, Master CSA II student

Abstract: *Insulin is the hormone indispensable for the body's energy and metabolic processes. In type I of diabetes, when insulin is no longer secreted by the pancreas, an external supply of insulin must be provided to the body, which will lead to a balance of blood glucose levels. In this paper, aspart insulin was taken in order to study the influence of storage conditions on its stability. Changes in insulin activity were observed by spectrophotometric measurements.*
Key words: *aspart insulin, absorption spectrum*

INTRODUCTION

Diabetes is a metabolic disease characterized by hyperglycemia (increased blood glucose), glycosuria (presence of glucose in urine), polyuria (consequence of osmotic diuresis caused by the presence of glucose in urine) and polydipsia (increased water intake)[1,2]. Diabetes (DZ) is of two types: DZ type I (insulin-dependent diabetes) and DZ type 2 (non-insulin-dependent diabetes, beginning on maturity).

A person with DZ type I has the inability to secrete enough insulin when eating, so the blood sugar level increases, which leads to high oscillations of blood glucose and also glycosuria appears if the glucose in blood exceeds 180 mg glucose / dl blood.

The treatment of DZ type I is done with insulin. Insulin classification is made according to their mode of action[3,4]. Thus, insulin differ from each other, depending on the start time of their hypoglycemic effect and on the duration of action.

Insulin synthesis has been continuously evolving. By modifying the sequence of certain amino acids in the structure of human-type insulin molecules, prepared insulin known as analogues have been obtained.

A fast-acting analogue insulin is NovoRapid (NR), which starts to act about 10 minutes later after subcutaneous administration. The duration of action is up to 5 hours, but the maximum intensity of action is recorded for 1-3 hours. The active substance is insulin aspart, and the other components are phenol, glycerol, metacresol, sodium chloride, zinc chloride, disodium phosphate dihydrate, sodium hydroxide, hydrochloric acid and water. It is found in 3 ml cartridges as solution for injection. Until use, it is advisable to keep it in the refrigerator at 2-8°C, and during the use it should be kept at a suitable temperature, not to exceed 30°C.

EXPERIMENTAL

In order to determine the influence of storage conditions on the activity of NovoRapid (NR), several insulin samples were used. Spectrophotometric analyzes[1] were performed on the UV-VIS SPECORD 210 PLUS spectrophotometer.

NR insulin samples which were kept under different storage conditions had been used, recording for each, the absorption spectrum. Subsequently, absorption spectra were recorded after the aspart insulin was exposed directly to the heat of the summer sun and to the ultraviolet radiation generated by the UV lamp.

Insulin samples of NR from three cartridges were taken from the cartridges and subsequently inserted into quartz tanks and subjected to spectrophotometric analysis[5]. Sample 1 of the NR belongs to a sealed cartridge, in the middle of the warranty term, which was kept in the refrigerator, at the temperature mentioned in the instructions in the package leaflet.

Sample 2 of NR was taken from an insulin cartridge, which was within the warranty period, but was not kept in the refrigerator all the time, and sample 3 of NR was from an expired insulin cartridge.

Another series of determinations concerned the absorbance changes of sample 1 of aspart insulin, which was maintained in unproper conditions. So, insulin from sample 1 was kept in the sun for three hours and also insulin from sample 1 was exposed to ultraviolet radiation for 90 minutes, respectively 180 minutes. After each exposing time in the ultraviolet lamp the sample was spectrophotometric analyzed.

RESULTS AND DISCUSSION

The absorption spectra of samples 1, 2, and 3 of NR insulin are shown in Figures 1-3. The result of the spectrophotometric analysis of the sample exposed to sun is presented in Figure 4.

The results of the spectrophotometric analyzes of NR sample 1 exposed to ultraviolet radiation at two different times are illustrated in Figures 5 and 6.

Analyzing the absorption spectra of Figures 1-3, it may be concluded that the maximum absorbance (Amax = 2.7156) is recorded in the case of insulin that falls within the validity period and has been stored properly. In the case of the insulin sample that was not stored according to the indications, the spectrum is similar, but the maximum absorbance is 1.9578, and in the case of the expired sample the spectrum shows a different appearance, in the form of a plateau with values close to 1.5 corresponding to the range of wavelengths 280-320 nm.

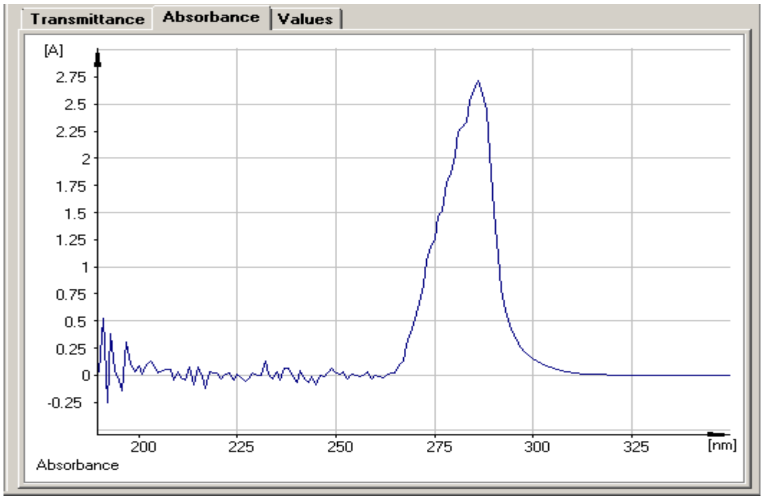

Figure 1. The absorption spectrum of sample 1 of NR

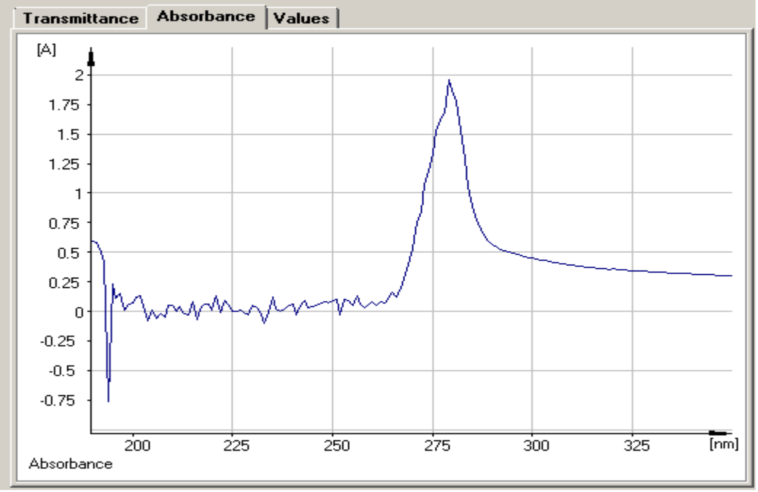

Figure 2. The absorption spectrum of sample 2 of NR

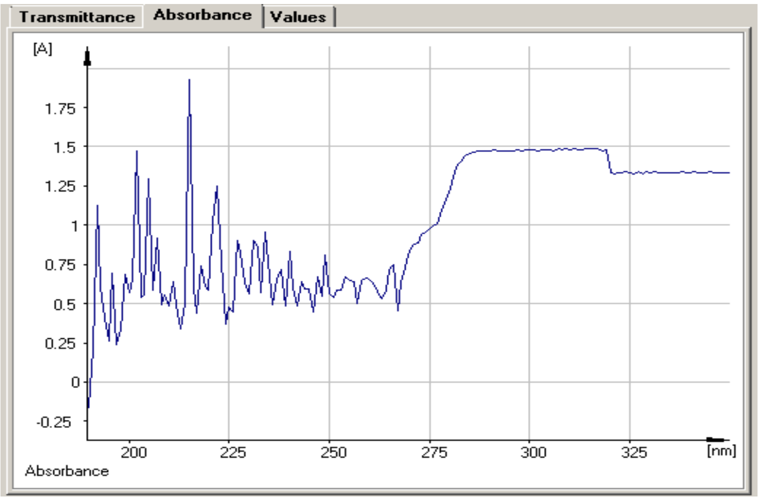

Figure 3. The absorption spectrum of sample 3 of NR

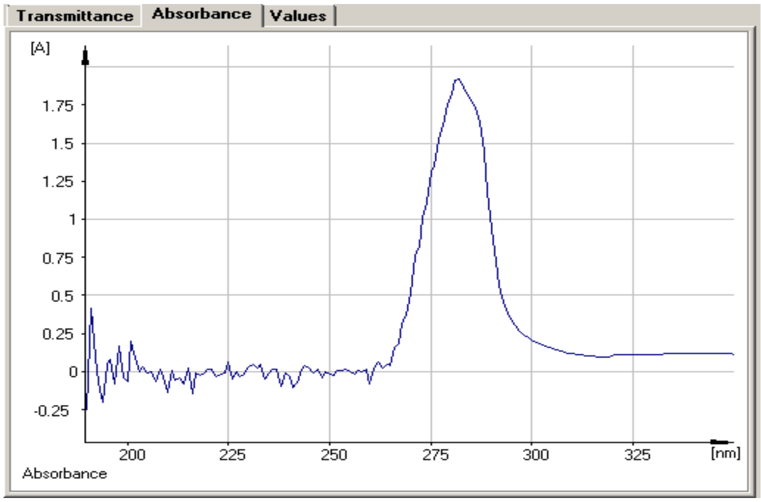

Figure 4. Absorption spectrum of sample 1, after 3 hours sun exposure

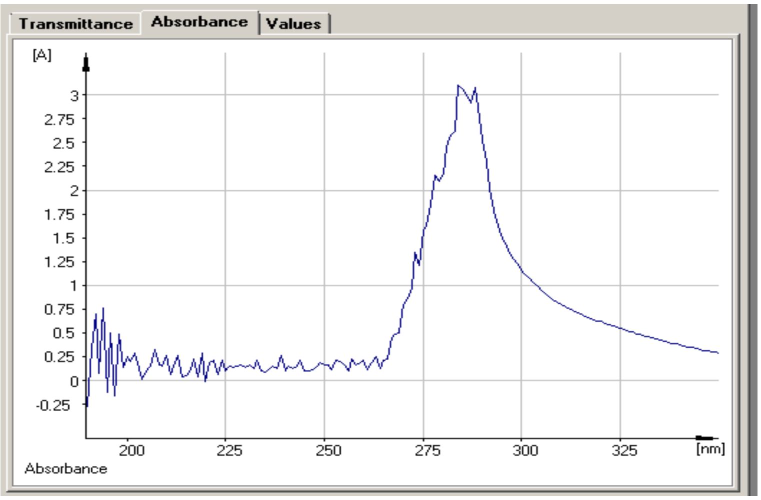

Figure 5. The absorption spectrum of NR sample 1, exposed to UV radiation for 90 minutes

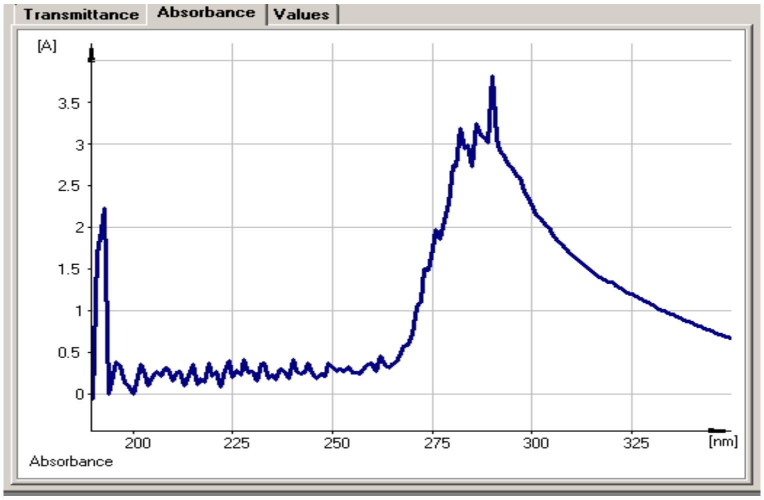

Figure 6. The absorption spectrum of NR sample 1, exposed to UV radiation for 180 minutes

Figure 4 shows the same shape of spectrum like those from figure 1, but the maximum absorbance has a lower value, 1.8302, compared to the initial value.

Analyzing Figures 5 and 6 you may notice that the maximum of absorption for the NR samples 1 exposed to ultraviolet radiation correspond to higher values of the absorbances compared to the NR sample 1 before UV exposure (Figure 1). At the same time, the allure of the spectra is different from the spectrum of the initial sample.

CONCLUSIONS

A compound of wide applicability in medicine is NovoRapid Insulin. This is an insulin that is absorbed rapidly, enters into action about 10 minutes after administration, being used in the treatment of type I diabetes (insulin-dependent), being administered before meal or immediately after, helping to remedy the acute metabolic imbalance. Laboratory analyzes of the possible modification of its activity according to certain factors were performed by spectrophotometric measurements.

For the correct application of insulin, it is compulsory for it to be within the shelf life mentioned on the cartridge and it must be kept cold to prevent its activity from decreasing, a fact proven by decreasing the maximum absorbance. In case of sun exposure, it has also been shown that insulin activity will decrease, being noticed a lower value of the absorbance compared to the sample kept under normal conditions.

In the situation of exposing to ultraviolet radiation, insulin changes its structure, which is evidenced by the increase of absorbance with the increase of the exposing time, but also by the spectrum, that has a different shape, which means that the activity of insulin is altered and can be harmful to the body due to the secondary products.

REFERENCES

[1] Cărăban, A. (2007). Biochimie metabolică– Lucrări practice, Editura Universităţii din Oradea

[2] Cărăban A. (2006). Biocatalizatori şi cinetică enzimatică, Editura Universităţii din Oradea, ISBN (13) 978-973-759-083-1.

[3] Magyar, I. (2011). Elemente de farmacologie fundamentală, farmacologie clinică şi toxicologie clinică, Editura Universităţii din Oradea.

[4] Perciun, R. (2005). Tratamentul diabetului zaharat, Editura Saeculum Vizual Bucureşti.

[5] ***, (2017). Farmacopeea Română, Editura Medicală, Bucureşti, Ediţia a X-a, ISBN 978-973-39-0662-9.

Analele Universităţii din Oradea-Fascicula Chimie, Vol. XXVI(26), 2019

INFLUENCE OF CHEMICAL AND MECHANICAL FACTORS ON S235 STEEL CORROSION IN ACID MEDIA

Gabriela Elena BADEA[1], Caius STĂNĂŞEL[2]
[1]University of Oradea, Faculty of Informatics and Sciences, ROMANIA, gbadea@uoradea.ro
[2]University of Oradea, Faculty of Informatics and Sciences, Chemistry III-student

Abstract

Modern technology has a wide range of construction materials available: metals, metal alloys, plastics, ceramic products, etc. Choosing the right material for the making of a given machine is a major responsibility of the specialists, a decision that can be taken only taking into account the chemical, physical and mechanical properties, but especially the effect of the interaction of the material with the environment in which it will be exploited, that is, the behavior at corrosion. S 235 steel is one of the cheapest and most widely used iron alloys. In the paper, the corrosion resistance of S 235 steel was estimated quantitatively and qualitatively, depending on different chemical and mechanical factors in HCl environment.

Key words: corrossion, inhibitors, acid media, surface roughness, electronic microscopy

INTRODUCTION

The process by which a metal or alloy is transformed from the metallic state to that combined by interaction with the environment, is called corrosion. The negative effects of corrosion are metal losses, respectively pollution with different metals, which by corrosion, contaminate water, soil or air. [1-9].

The corrosion process is a redox reaction, which occurs at the metal / solution interface, with electron transfer through metal and ion transport through solution, a process that includes

- oxidation (electron-transfer) reaction of the metal:

$$M \rightarrow M^{z+} + ze^-$$

- reduction reaction (electron acceptance) of an acid depolarizer from acid environment:

$$H^+ + e^- \rightarrow H \rightarrow \frac{1}{2} H_2$$

The two processes, metal oxidation and depolarizing reduction are carried out at equal speeds, at the same potential, called corrosion potential. The corrosion can have characteristic aspects and depending on the size of the attack surface.

- general corrosion, on large surfaces, and where the attack is somewhat uniform;
-localized corrosion, which occurs on very small surfaces, but where the attack is very intense, the causes being the physical or chemical heterogeneities of the electrode / electrolyte system.

EXPERIMENTAL

The metal samples made of carbon steel S 235 were studied in 1N HCl, under static conditions, at 20 ° C, in the absence and presence of a corrosion inhibitor, K2Cr2O7, 1% solution.

The tests under static conditions were carried out in 100 ml Berzelius glasses. The mechanical processing of the carbon steel samples, in order to obtain different asperities, was done by milling with the help of the Mill Concept 55 numerical control mill.

The metal samples were degreased with soda and dried with filter paper, then weighed at the analytical balance with an accuracy of 0.0001g .

After removing the samples from the solution, they were washed with 10% ammonium citrate solution, to remove corrosion products, then with distilled water and dried.

The evaluation of the corrosion resistance of S 235 steel was made by the gravimetric method, following which were determined:

-the gravimetric index, which represents the variation of the sample weight (Δm), as a result of corrosion, in the time unit, (t) and on the surface unit (S) [1,2]:

$$v_{cor} = \frac{m_i - m_f}{S \cdot t} \quad (g/m^2h) \qquad (1)$$

-the penetration index (depth), given by the relation:

$$P = \frac{v_{cor}}{\rho} \cdot 8{,}76 \quad (mm/year) \qquad (2)$$

The penetration index is closer to the practice than the gravimetric index and allows the estimation of the operating time of the machines.

RESULTS AND DISSCUSIONS

Influence of chemical factors of S 235 steel corrosion in HCl 1N

Table 1 shows the corrosion rates and penetration rates, calculated with the relations (1) and (2), in 1N HCl at 25ºC, under static conditions, after 1 and 7 days respectively.

The steel samples had an area of S = 0.002 m^2.

Tabel 1. Evaluation of corrosion rate of S235 steel in HCl 1 N

Sample	m_i(g)	m_f(g)	t (h)	v_{cor}(g/m^2h)	P(mm/an)
I (HCl)	7,52	7,0249	24	10,310	11,505
III (HCl)	7,47	7,1315	168	1,0074	1,124

Tabel 2. Evaluation of corrosion rate of S235 steel in HCl 1 N in the presence of the inhibitor.

Sample	m_i(g)	m_f(g)	t (h)	v_{cor}(g/m^2h)	P(mm/an)
II (HCl +inh)	7,46	7,3568	24	2,1500	2,390
IV (HCl +inh)	7,42	7,3433	168	0,2282	0,254

The obtained results are compared with the values of the corrosion resistance rating scale [2]. From the point of view of the value of the corrosion rate: the behavior of carbon steel in 1N HCl belongs to the category of stable metals, well usable. From the point of view of the penetration index, however, carbon steel in 1N HCl is bounded between the somewhat resistant metal groups.

These results indicate that it is advisable to apply an anti-corrosion protection method, even if corrosion rates and penetration rates are not very high, such as the use of corrosion inhibitors.

There is a decrease of almost an order of magnitude by the measured values after one day and comparable values, but smaller in case of use of the inhibitor, after 7 days. These values attest that in the case of chemical conditioning of the environment, by using a corrosion inhibitor, according to the rating scale, carbon steel passes into the very stable metal class at corrosion.

Qualitative methods for corrosion evaluation

The most widespread is visual examination, based on the observation with the open eye or the magnifying glass of the external aspect of the sample, that is to say, the appearance and distribution of corrosion products. Figure 1 shows comparative photographs of the control and corroded samples.

Figure 1.Photographs of the control sample and of the corrosion samples after 1 day, respectively 7 days in 1N HCl, a) Control sample, I, III, b) 1 day (I) in HCl , c) 7z (III) HCl cleansed of oxides.

The visual method allows to characterize the type of destruction: a uniform corrosion is observed on the surface inside the solution, where a gray-black layer appears, corresponding to the passive oxide layer and a non-uniform corrosion on the surface outside it, with reddish surfaces - Fe_3O_4 (rust) and green -$Fe(OH)_2$ and where the localized pitting (dots) and crevice forms, which are produced by the differential aeration mechanism, are visible.

However, the presence of Cl^- ions makes their presence felt, being well known their role in initiating and propagating pitting on metals covered with passive layers.

The examination with the electron microscope allows the observation of the modifications made in the structure of the metal as a result of structural corrosion, intercrystalline - corrosion crevices and transcrystalline - corrosion points (pitting).

Examination with the electron microscope allows to evaluate the thickness of the corrosion products, the depth or surface of the corrosive attack in the case of pitting.

Figure 2 shows comparatively a microscopy of the control sample, cleaned with abrasive paper and sample 1, with the smallest roughness, at 3 resolutions: x100, x200, x500.

Influence of mechanical factors of S 235 steel corrosion in HCl 1N

The anticorrosion methods, through the action on the construction material, concern two aspects:

- rational choice of the material, with good corrosion resistance,
- further processing of the material - to reduce the possibility of corrosion occurring, such as by ensuring a more homogeneous structure.

It is well known that any chemical, physical or mechanical heterogeneity is an initiating factor of the appearance of corrosion, through its different mechanisms, general or localized.

Figure 3 shows the metal samples S 235 subjected to mechanical processing, after which the surface presented different roughness.

The surfaces subjected to corrosion were obtained by mechanical machining by milling, using a three-toothed cylindrical-front mill and the cutting regimes listed in Table 3.

Table 4 compares the results obtained by electron microscopy, by exposing, for one hour, the attack of a drop of 1N HCl to four samples from S 235, whose surface had different roughness.

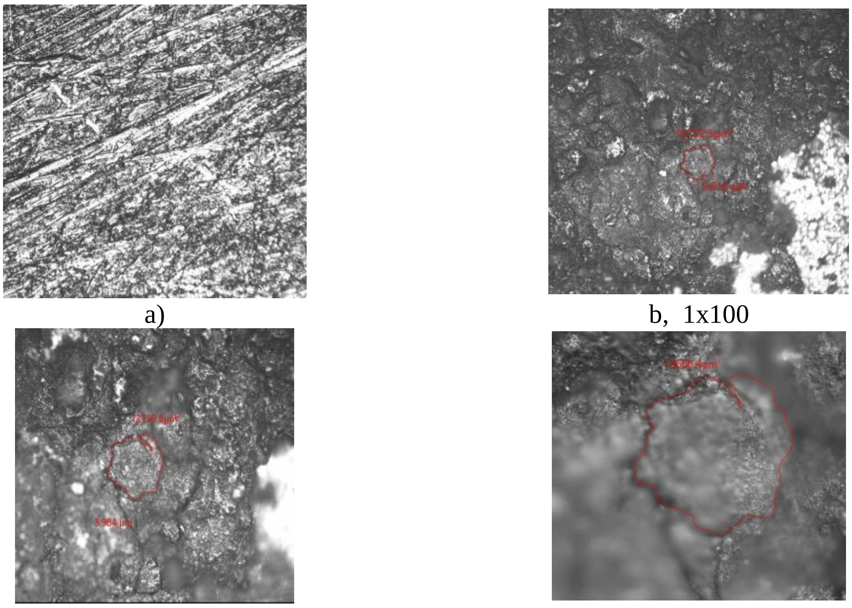

a) b, 1x100

b,1x200 b, 1x500

Figure 2. Electron microscopy, a) for the blank sample, processed with abrasive paper and the sample b) -sample 1- mechanically processed, at resolutions x100, x200, x 500.

Table 3.Characteristics of the mechanical machining used for milling.

Sample / Parameter	Sample 1	Sample 2	Sample 3	Sample 4
Speed, n, [rot/min]	3500	3500	3500	3500
Working advance, v_f, [mm/min]	300	600	700	800
Cutting depth, a,[mm]	0,5	0,5	0,5	0,5
Roughness, R_a, [µm]	1,596	1,720	1,736	1,894

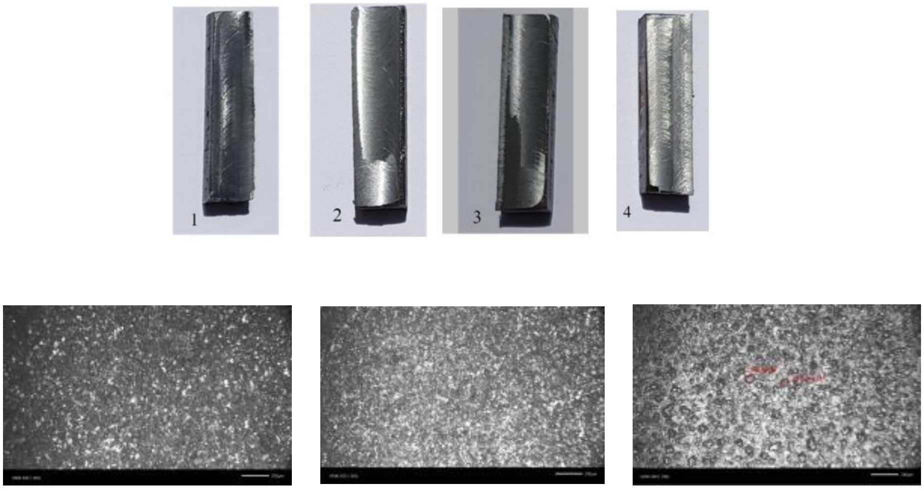

1 x100

Figure 3. Milling samples : photos and x100 electron microscopies.

Table 4. Electron microscopy, x 200 - Pitting surface variation with degree of surface processing (S 235 treated with 1N HCl)

Sample 1	Sample 2	Sample 3	Sample 4
Roughness Ra=1,596 [µm]	Roughness Ra=1,720 [µm]	Roughness Ra=1,736 [µm]	Roughness Ra=1,894 [µm]
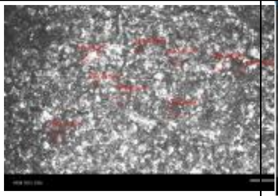	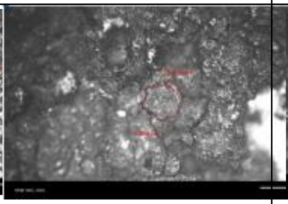	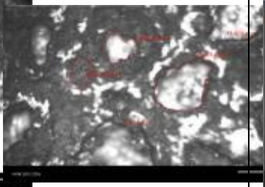	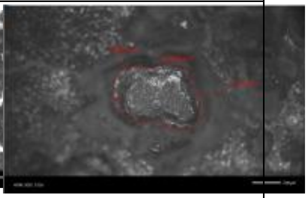
S=0,000569– 0,001554 [mm$^{2]}$	S=0,012130 [mm^2]	S=0,029369 [mm^2]	S=0,21698 [mm^2]

An increase in the surface dimensions of the corrosion pitting, as well as the depth of the pitting, is observed, as the surface non-uniformity / roughness increases.

CONCLUSIONS

In conclusion, following the results obtained in the study of steel corrosion in 1N HCl environment, in the absence and in the presence of the corrosion inhibitor, K2Cr2O7 1%, the following can be stated:

- S 235 carbon steel in HCl medium in the absence of the inhibitor is somewhat stable at corrosion;

- the influence of the chemical factor, by the presence of the corrosion inhibitor-K2Cr2O7, makes the carbon steel S 235 in 1N HCl environment, become very stable at the corrosion;

- the influence of the mechanical factor of processing of the exposed surface indicated a more intense corrosive attack in case of a greater uniformity / roughness, due to the intensification of the corrosion forms localized by the mechanism of the differential aeration.

In assessing the corrosion stability of a metallic material, all factors must be taken into account: chemical, physical and mechanical and the fact that the measurements in static laboratory conditions can differ significantly, in a negative sense, from the dynamic, real conditions of operation of a metal. machine or plant.

This complex aspect emphasizes the importance of interdisciplinarity in the preparation of any engineer.

REFERENCES

1. G.E.Badea,(2007): Chimie şi Coroziune, Ed. Universităţii din Oradea.
2. G.E.Badea, D.Ionita, P.Cret, Corrosion and passivation of 304 stainless steel in formic acid solutions, Materials and corrosion, 2014, vol.65, nr.11, pg.1103-1110.
3. G.E.Badea, S.Dzitac, C. Porumb, L.Popper, T.Badea, Nitrate ion effects on the nickel corrosion and passivation behaviour in 0.5 M H2SO4 solutions, Revue Roumaine de Chimie, 2010, 55(4), pg, 263-267.
4. G.E.Badea, T. Badea, “Electrochemical behaviour of Ni in aqueous acetic acid solutions’, Revue Roumaine de Chimie, 2008, *53*(4), 291–295.
5. G.E.Badea, T.Badea, *Anodic behavior of nickel in 1N solutions of sulphuric, formic, acetic, oxalic and citric acids*, Rev. Roum. Chim., , pg. 671-675,50(7-8), 2005.
6. G. E. Badea, A. Cojocaru and T. Badea*“ Nickel anodic behaviour in formic acid solutions”,* Rev. Roum. Chim., pag.141-146, 50(2), 2005.
7. G.E.Badea, T.Badea, C*orrosion and passivation behaviour of the 18Cr/10Ni stainless steel in 1N* H_2SO_4 *solutions, in the presence of oxalate and tartrate anions*, Rev. Roum. Chim.,, pg. 689-694 ,50(7-8), 2005.

8. G.E.Badea, A.Cojocaru, T. Badea, “C*orrosion and passivation behaviour of the 18Cr/10Ni stainless steel in 1N solutions of formic, acetic, oxalic and citric acid*” Revista de Chimie, pg.1029-1030,55, 12, 2004.

9. T.Badea , G.Badea, A.Cojocaru, “*The inhibition action on mild steel corrosion in 1M HCl of some aliphatic and aromatic aldehydes. Effect of inhibitor concentration and medium temperature”* Rev. Roum. Chim., pg. 37-47 , 49(1), 2004.

THE SEPARATION OF CAROTENOIDS FROM ROSE PETALS BY TLC

Sorin HODISAN[1]; Mioara SEBESAN[1]
[1]University of Oradea, Faculty of Informatics and Sciences, Romania

Abstract: *Carotenoids are plant pigments spread in plant tissues and animals. These pigments print yellow, red or blue color, tissues that were. In herbal the carotenoids was in leaves, fruits, stems, roots, seeds, petals and in pollen. Amount of carotenoids in dried leaves is between 250-650 mg/g. Carotenoids pigments are synthesized only of vegetable. Carotenoids have practical applications in medicine and cosmetics and their use as food additives, dyes and antioxidants.*

Key words: carotenoids, leucina, tirozina, luteina, zeaxantina, β-criptoxantina ,TLC, Silica gel

INTRODUCTION

Carotenoids along with flavonoids and isoflavones are biological substances, called phytochemicals („phyto" means „from herbals") which give the flavor, aroma and resistance to the disease having an important role in photosynthesis and photoprotection . Food consumption rich in β – criptoxantina, carotenoid a color orange – red significantly decreases risk of lung cancer, according to a study published in 2003 in „Cancer Epidemiology, Biomarkers and Prevention"magazine[1] .

Analysis of carotenoids from plants was inserted by Tswett (1906), subsequent findings, identification and elucidation structure have been developed by Karrer, Zechmeister, Talerand, Goodwiszi [2-5]. Curent methods for operation and analysis carotenoids includes new methods separation as TLC and HPLC to replace or complementary with classical technique (locked column chromatography) [6-8]. „

There is limited on composition carotenoids from the rose petals separated by open column chromatography. Purpose of this study is characterizing the type of carotenoids from rose petals using methods of separation (TLC, HPLC) to identify major components.

EXPERIMENTAL

Solvents used in chromatographic separation are of analytical purity (methyl acetate, hexane, chloroform, acetonitrile) or distilled (acetone, ethyl ether, ethanol) and as buffer substances use : TEA and antioxidants (butylated hidroxytoluene – BHT).

The rose petals were dried at room temperature in airflow about 5 – 6 days, have shelled and after which the maceration. Seeds macerated dry in oven about 3 hours, then are crushed in mortar to reach as a powder. The powder to be extracted with chloroform : ethanol : petroleum ether (3 : 2 : 1 v/v/v) for 10 hours at dark to prevent degradation and oxidation of carotenoids. Crude extract filtered, evaporate to drying in Rotovapor and re – suspended in ethyl ether.

Saponification was done in ether being added to 25% KOH in ethanol until the final concentration of 10% V/V KOH. Mixture was stirred with a magnetic stirrer for 6 hours, carotenoids being extracts for 3 – 4 times successively with ethyl ether a solution with neutral pH.

Soap is removed, extract all the carotenoids was evaporated with Rotovapor, brought to a certain volume and used for chromatographic separation.

The total concentration of carotenoids of total extract (TE) is calculated by comparing absorbance A (α_{max} = 450 nm) with a specific absorbing (α = 400 nm).

$$X = (A \times Y \times 1000) : (2500 \times 100)$$

$$= A \times Y / 250$$

Where:

X – weight carotenoids of sample (mg)
Y – sample volume (ml)

To characterize the composition in carotenoids of rose petals has made a preliminary separation total extract (TE) on a column of alumina (Al_2O_3 with 5% water). Small volumes were taken of total extract and were placed on the column and eluted with 3 solvent systems:

- 100% petroleum ether (fraction 1)
- petroleum ether : ethyl ether (1 : 1 v/v) (fraction 2)
- ethanol in ethyl ether 5% v/v (fraction 3)
-

Total extract and fractions 1 – 3 released from the alumina column were separated on silica gel plates (SilG, Merk) and chromatograms were analyzed in Shimadzu CS – 5000 with beam with dual wavelength. For total extract used a separation of two stages:

- with 20% v/v acetone in petroleum ether
- with 100% petroleum ether

For fractions 1 – 3 developing systems was:

- 5% v/v acetone in petroleum ether (fraction 1)
- 10% v/v acetone in petroleum ether (fraction 2)
- 15% v/v acetone in petroleum ether (fraction 3)

RESULTS AND DISCUSSIONS:â

Total extract has undergone quantitative analysis. Peakurile obtained of densitograma TLC (figure 1) recorded at 450 nm have been identified and compared with total extract, with separation standard (S) same conditions. Major carotenoids identified were: leucine, tyrosine.

Fraction 1 contains 2 main peakuri results of TLC separation representing non – polar carotenoids (leucine and tyrosine ;).

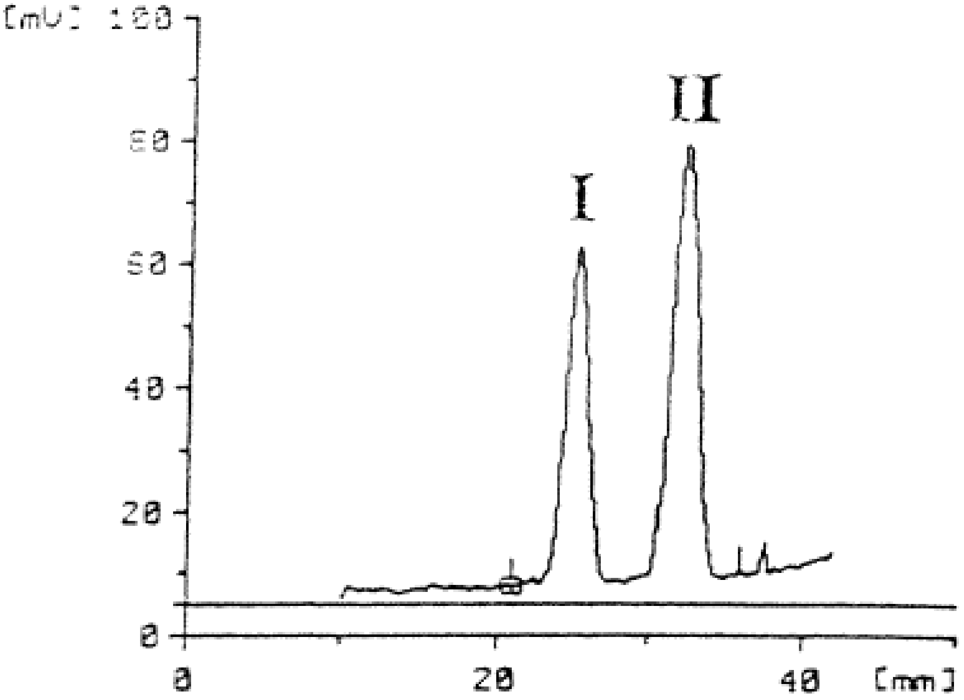

Figure 1. TLC chromatogram the total extract: 1-leucine; 2-tyrosine;So we learned only percentage composition the main carotenoids in extract and not in their absolute: 26,46% leucine; 21,30% tyrosine; Fractions 1 collected from alumina columns were analyzed by TLC.

4.CONCLUSIONS

Total amount of carotenoids from rose petals assessed by spectrometry in the VIS the total extract was 80 mlg^{-1} dry mass.

By chromatographic analysis (TLC) have highlighted the main carotenoids present in rose petals: leucine, tyrosine, in total extract distributed differently between fractions diluted of alumina column. TLC proved a rapid and useful method for separation of carotenoids from rose petals.

REFERENCES

[1] Cancer Epidemiology, Biomarkers and Prevention"magazine, 2003,pp. 138 – 145.
[2] Gross,J. (1995) „„Pigments in Fruit", *Academic Verlang, Basel*
[3] Isler, O. (1971), "Carotenoids", *Birkhauser Verlag, Basel*, pp.773 – 791.
[4] Goodwin,T.W., Trevor,W., (1994), *J. Plant Phisiol*, 143, pp. 440 – 452.
[5] Neamtu,G., Tamas,V., (1986), "Pigmenti carotenoidici si metabolite",vol. 1-2, *Ed. Ceres, Bucuresti.*
[6] Phander,H., Riesen,R., Niggli,U., (1994), *Pure Appl. Chem.*, 66, pp. 947 – 955.
[7] Phander,H., Socaciu,C., Neamtu,G., (1994), *Studia univ.Babes-Bolyai, Cluj-Napoca*, chemia vol. 1-2, pp. 71-77.
[8] Meyer,V.R., (1988), *Practical High-Performance Liquid Chromatography,Wiley Chichester*, 4-8 and 80-117.

Analele Universităţii din Oradea-Fascicula Chimie, Vol. XXVI(26), 2019

CHEMICAL IMPACT OF POWER INDUSTRY ON THE ENVIRONMENT

Nicolae HODUȚ[1], Gheorghe-Constantin IONESCU[2], Gabriela Elena BADEA[2], George Lucian IONESCU[2], Petru CREȚ[2]

[1]University of Oradea, Romania, PhD-Student
[2]University of Oradea, ROMANIA, gbadea@uoradea.ro

Abstract.
A living world is impossible without energy. But the developed world must work to ensure that the economies do not add to the world's environmental problems. People have to become conscious about the risks of power production and learn new ways and strategies to protect the environment. Green energy is a solution, but sometimes even renewable sources are not so green. The most important issues of chemical impact of power industry on the environment are presented.The results of the risk analysis are important to find out the consequences on the emergency situation that may occur.

Key words: chemical risk analysis, environment, power industry

INTRODUCTION

Most air pollution comes from one human activity: burning fossil fuels—natural gas, coal, and oil—to power industrial processes and motor vehicles. When these fuels are burnt, the energy released can be harnessed to produce electricity, power vehicles, heat industry and homes, cook food.

Pollution, in general, and chemical pollution in particular, is a complex phenomenon, by which substances accidentally arrived, but especially artificial in the environment, they worsen the quality of the environmental factors [1,2].

With the development of industry and technology, the effects it has on people and environment has made it necessary to make a more systematic approach to preventing, limiting and combating chemical or other pollution. The energy industry is an important source of pollution through all its elements: energy resources, production, transport, distribution and consumption of energy. But the share of pollution is the most important power plants.

The main forms of pollution produced by energy installations are: chemical pollution, thermal pollution, noise pollution, electromagnetic pollution, radioactive pollution, aesthetic pollution. Chemical pollution in the energy field can be classified according to the appearance of pollutants in the environment:

- directly - due to the evacuation in the natural circuit (air, water, soil) of the products resulting to the combustion of fuels, of some chemical substances used in the technological process or of the raw material itself, coal, crude oil, gas, biomass.
- indirectly - through the resulting products from the manufacture of the component elements of the installation or the exploitation of the installation (corrosion), transport, etc.

EXPERIMENTAL

A hazard analysis is used the first step in order to assess a risk. From the hazard analysis results the identification of different hazard types .A hazard represents a potential positive or negative condition (probability is 1 or 0), and alone or with other hazard conditions could become a Functional Failure or Accident. The particular way this exactly happens is named a "scenario", with a probability of occurrence (between 1 and 0). Different systems could have different potential failure scenarios, classified function of the case severity. More precise prediction and acceptance of risk could be determined in the Risk Assessment Analysis [3,4].

The main goal of both analysis is to give the best way for controlling or eliminating the risk and the method could be applied in many engineering specialties: chemical process safety, safety engineering, reliability engineering or food safety[3,4].

RESULTS AND DISCUSSIONS

The chemical pollution resulting from the power industry affects the air, water and soil. Table 1 presents the main chemicals that pollute the air. In table 2 are presented some chemical substances that are constituted as sources of artificial pollution.

Table 1. The main chemical air pollutants in the power and adjacent industries.

Pollutant	**Source**
CO_2, CO, SOx, NOx, powders, N_2O, O_3, volatile organic compunds (VOC);	Burning of fossil fuels (coal, petroleum products, natural gas), power plants
(CO, NOx), N20, powders, COV, Pb, SOx,	Transportation
COV, NOx, SOx	Petrochemistry
Hidrocarbs	Extraction, transport and distribution of oil, petroleum products and natural gas

Table 2. Substances present in wastewater from the power and adjacent industries.

Pollutant	**Source**
Ammonya	Cokechemical plants
Fluorides	Nuclear power plants
Cianides	Metal coatings, metal cleaning
Acids	Mines, drilling, cleaning solutions for plants, thermoelectric power stations, accumulators
Cr, Zn, Ni, Cd, Cu	Metal coatings
Fats, oils	Oil refineries
Fenols	Cokechemical plants
Hidrocarbs	Petrochemical installations, thermoelectric power stations
Metal ions	Corrosion of metallic structures and pipes
Mercaptans	Oil refineries

Some of the air pollutants form acid rain and reach the water and soil. Soil is the environmental factor that integrates all the consequences of pollution, making it the most difficult to pollute.

Acid gases (SO2 and NO2), released by burning fossil fuels, are deposited on the ground, by dry or wet deposition and can increase its acidity, causing disruptions to its regeneration processes, changing its composition, releasing metal ions (eg Al), with negative effects on vegetation and on groundwater

The primary and secondary pollutants, due to the functioning of the thermal power plants, are among the main pollutants with negative effects on the construction materials: SO2 and sulphates, NOx, and nitrates, CO and O3 and VOC, leading to surface erosion, cracking, crust formation, dirt , corrosion.

Soil pollution is the most complex, since the soil is not a homogeneous environment. The soil is difficult to clean and can last for long periods.

Table 3 presents the most important chemicals in the energy industry that pollute the soil. Table 4 presents the main chemical pollutants from the energy industry that affect human health.

Table 3. The main chemical soil pollutants in the power and adjacent industries.

Pollutant	**Source**
Oil spills, salt water and well mud	Extraction wells, refineries, transport, power plants and district heating
Powders, metal oxides, ash, slag	Thermal installations, thermoelectric power stations
Waste, residues	Thermal installations, thermoelectric power stations
Radioactive waste	Nuclear Plant
Coals	Storage dumps

Table 4. Chemical pollutants in the power industry that affect human health.

Pollutant	**Source**
Suspension powder	power plants and district heating, coal burning stoves
CO_2, CO, SOx, NOx, powders, N_2O, O_3, volatile organic compunds (VOC);	power plants and district heating, coal burning stoves

All these chemicals are potential risks for the environment, for human health, for the safety and security of work in the energy and adjacent industries, which makes not only interesting, but absolutely necessary a risk analysis, at the level of any industrial objective, all the more so. in the vital and complex field of energy. in order to be able to prevent, limit, eliminate their consequences.

To determine the chemical risks the method of Hazard analysis and risk assessment is ussualy used. This method includes several steps: the description of the system, the hazard analysis, the risk assessment, the risk rating and the risk resolving.

In table 5 is presented a simplified hazard analysis for a combined heat power plant.

As noted, air pollution is one of the most serious problems, in the short and medium term, in terms of health. Polluted air is more difficult to avoid than polluted water. Its effects, which penetrate everywhere, damages the health, degrade the constructions and the natural medial. Solving the problem of atmospheric pollution must be the top priority for the environmental protection policy, within the thermoelectric power stations.

Also, the knowledge of the properties of the raw materials, as well as of the construction materials of the installations, the knowledge of the physico-chemical processes involved, requires an interdisciplinary analysis in the analysis of the potential risks.

Table 5. Chemical hazard in various operational area of a power plant .

Hazard	**Cause**
Respiratory problem	very fine coal dust
Chemical burn	Spillage of caustic soda lye and sulphuric acid during unloading, pipe damage or overflow
Fire/explosion	Damage or incorrect handling of equipment, disregard of the chemical properties of the materials involved
Eye irritation and respiratory problem	exposure to other chemical substance’s leakage

CONCLUSIONS

The pollutants generated by the energy industry using conventional energy sources (coal, crude oil, natural gas) are virtually unknown, but what is more important are the implementation of methods of prevention and protection of the environment.

Neither the impact on the environment produced by other green energy sources, the renewable energy sources that contribute to the chemical pollution of the environment either directly (biomass) or indirectly and can also have a specific impact on the environment should not be neglected.

Risk assessment is useful for identifying hazards at the plant level. Hazards must be analyzed and evaluated in order to prioritize, in order to prepare urgently and maintain a safe workplace.

Resources are often limited, so it is important to know the various risks and their incidence, in order to establish rules of action. The results of the risk analysis are important to find out the consequences on the emergency situation that may occur. For an effective response, measures can be taken to limit the risks, limit the consequences of an accident and to train and improve the training level of the personnel involved,

In order to ensure the access and the satiation of the energy needs, an integrated approach in the field of energy resources is needed for greater energy security, a strategy to identify the major risks and threats in the energy field, to establish achievable objectives and action directions that to lead to a high level of energy security in the medium and long term.

REFERENCES

[1] V.Rojanschi, F.Bran, G. Diaconu, Protectia si Ingineria mediului, Editura Economica, Bucuresti, 1992.

[2]M. Negulescu, L. Vaicum: Protecţia mediului înconjurător, Ed. Tehnică, Bucureşti, 1995.

[3] Ravindra Rathod, Dr. G.D. Gidwani and Pulkit Solanky, Hazard Analysis And Risk Assessment In Thermal Power Plant, International Journal Of Engineering Sciences & Research Technology, 6(7): July, 2017.

[4] https://en.wikipedia.org/wiki/Hazard_analysis.

(12pt)

INSTRUCTIONS FOR AUTHORS (TIMES 14 PT BOLD, CAPITAL LETTERS, CENTRED)

(10pt)

First name SURNAME[1], First name SURNAME[2] (12 pt bold)

[1]Affiliations and addresses (10 pt)Affiliations and addresses (10 pt)

(10pt)

(10pt)

Abstract: *Abstract of 50-120 words (10 pt italic). It contains concise information about: objectives of the work, the results obtained, conclusions*

Key words: List 2-6 keywords. (l0 pt, italic).

(10pt)

(10pt)

INTRODUCTION (l2PT. CAPITAL, BOLD)

The paper has to be written in English. Each paper should be concise including text, figures and tables. Authors are kindly requested to submit a paper a hard copy or in electronic format in Microsoft Word file form. Acceptable versions are MS-Word 2003, 2007, 2010. The suggested structure of the main text: Introduction; Methods, Techniques, Materials, Study area; Results and Discussions; Conclusions; References. (10pt)

(10pt)

INFORMATION (12 PT CAPITAL, BOLD)

Page layout (10 pt, bold)

- Use A4 format (210 x 297 mm),
- Margins: Top – 2,5cm, Bottom - 3 cm, Left- 4 cm and Right - 3 cm
- Paragraphs: alignment - justified, line spacing – 1,
- Font style: Times New Roman.
- Text: l0pt.: regular, text in tables: 10 pt, 1 line space and centred, 2 columns,
- equations: Equation editor, 10 pt, centred,
- c*aption of tables and figures: 10 pt, italic*

All tables and figures follow the References or could be inserted within the text. Tables, together with figures should be placed in their order of appearance in the text. Tables should be numbered consecutively. Table captions containing the number of the tables, followed by the caption, and should be placed above the table. Tables should be clearly captioned and all symbols should be properly explained in either the table or its caption.

Figures (min. 300 dpi) can be in colour, but must also be clear enough for black and white reproduction. They should be centred and numbered consecutively and so referred to in the text. Each must be clearly captioned (after the Figure number) below the figure.

Equations will be centred and numbered consecutively (right aligned).

All references would be cited within the text as superscripts after the punctuation's marks.[1]

(10pt)

All papers cited should be listed under the **REFERENCES** (1 column), in order of appearence according to the author's last name. The list of references should follow the format given below:

(Journal Article)

[1] Abbott, M. B., Petersen, M. M., and Skovgaard, O. (1978). On the numerical modelling of short waves in shallow water, Jnl Hydraulic Res; Vol 16 (3), pp. 23-44.

(Report)

[2] Carter, B., and Connell, C. (1980). Moa Point Wastewater Treatment Plant and Outfall Study, Report for the Wellington City Council, Wellington, pp. 31.

(Book)

[3] Grady, C.P.L., and Lim, H.(1980). Biological Wastewater Treatment Theory and Application, Marcel Dekker, New York, pp. 375.